GRK2 mediates TCR-induced transactivation of CXCR4 and TCR–CXCR4 complex formation that drives PI3Kγ/PREX1 signaling and T cell cytokine secretion

Brittney A. Dinkel[‡§1], **Kimberly N. Kremer**[§], **Meagan R. Rollins**[§], **Michael J. Medlyn**[§], and **Karen E. Hedin**[§2]

From the ‡*Mayo IMM Ph.D. Training Program, Mayo Clinic Graduate School of Biomedical Sciences, and* §*Department of Immunology, Mayo Clinic College of Medicine and Science, Mayo Clinic, Rochester, Minnesota 55905*

Edited by Luke O'Neill

The immune system includes abundant examples of biologically-relevant cross-regulation of signaling pathways by the T cell antigen receptor (TCR) and the G protein–coupled chemokine receptor, CXCR4. TCR ligation induces transactivation of CXCR4 and TCR–CXCR4 complex formation, permitting the TCR to signal via CXCR4 to activate a phosphatidylinositol 3,4,5-trisphosphate–dependent Rac exchanger 1 protein (PREX1)–dependent signaling pathway that drives robust cytokine secretion by T cells. To understand this receptor heterodimer and its regulation, we characterized the molecular mechanisms required for TCR-mediated TCR–CXCR4 complex formation. We found that the cytoplasmic C-terminal domain of CXCR4 and specifically phosphorylation of Ser-339 within this region were required for TCR–CXCR4 complex formation. Interestingly, siRNA-mediated depletion of G protein–coupled receptor kinase-2 (GRK2) or inhibition by the GRK2-specific inhibitor, paroxetine, inhibited TCR-induced phosphorylation of CXCR4–Ser-339 and TCR–CXCR4 complex formation. Either GRK2 siRNA or paroxetine treatment of human T cells significantly reduced T cell cytokine production. Upstream, TCR-activated tyrosine kinases caused inducible tyrosine phosphorylation of GRK2 and were required for the GRK2-dependent events of CXCR4–Ser-339 phosphorylation and TCR–CXCR4 complex formation. Downstream of TCR–CXCR4 complex formation, we found that GRK2 and phosphatidylinositol 3-kinase γ (PI3Kγ) were required for TCR-stimulated membrane recruitment of PREX1 and for stabilization of cytokine mRNAs and robust cytokine secretion. Together, our results identify a novel role for GRK2 as a target of TCR signaling that is responsible for TCR-induced transactivation of CXCR4 and TCR–CXCR4 complex formation that signals via PI3Kγ/PREX1 to mediate cytokine production. Therapeutic regulation of GRK2 or PI3Kγ may therefore be useful for limiting cytokines produced by T cell malignancies or autoimmune diseases.

Abnormal expression of T cell cytokines is a prominent feature of immune dysregulation associated with many diseases, including autoimmune diseases and cancer (1, 2). T cell–mediated cytokine production critically regulates the differentiation and activation of innate and adaptive immune cells and directs the overall immune response (3). T cell–mediated cytokine production is extensively regulated. Previous studies have documented cross-regulation of signaling between the T cell antigen receptor (TCR)[3] and chemokine receptor CXCR4 that impacts key T cell functions such as T cell migration, development, and immune activation (4–11). In particular, the stimulation of either CXCR4 or TCR with their respective ligand results in the physical association of these two receptors and downstream signal transduction controlling cytokine production (10, 12). Although TCR and CXCR4 have been demonstrated to physically associate in response to TCR stimulation, the molecular mechanisms required for the TCR-mediated CXCR4 transactivation and TCR–CXCR4 complex formation responsible for controlling robust cytokine secretion by immune-activated T cells have not been characterized.

TCR recognition of its cognate antigen/MHC ligand results in the activation of multiple signaling pathways that result in T cell proliferation and cytokine production (13). The TCR consists of six noncovalently-associated polypeptides: the variant αβ-subunits that dimerize to form the ligand-binding site of the receptor, and the invariant signal-transducing subunits CD3-ε, -δ, -γ, and -ζ (14). Upon TCR recognition of its cognate antigen/MHC ligand, TCR receptor-associated intracellular tyrosine kinases such as Src kinases and ZAP-70 are activated and initiate multiple signaling pathways that drive T cell proliferation and cytokine production (14). Another receptor that reg-

[3] The abbreviations used are: TCR, T cell antigen receptor; GPCR, G protein–coupled receptor; PI3Kγ, phosphatidylinositol 3-kinase γ; PLA, proximity ligation assay; MHC, major histocompatibility complex; RTK, receptor tyrosine kinase; MAPK, mitogen-activated protein kinase; GRK, G protein–coupled receptor kinase; PIP$_3$, phosphatidylinositol (3,4,5)-trisphosphate; YFP, yellow fluorescent protein; CFP, cyan fluorescent protein; PBMC, peripheral blood mononuclear cell; EGFR, epidermal growth factor receptor; IL, interleukin; IFN, interferon; qRT, quantitative RT; DAPI, 4′,6-diamidino-2-phenylindole; eGFP, enhanced green fluorescent protein; mAb, monoclonal antibody.

ulates TCR-mediated cytokine production is the G protein–coupled receptor (GPCR), CXCR4. CXCR4 is a chemokine receptor that regulates migration of both naive and activated T cells in response to CXCL12 (15, 16). Previous studies from our laboratory have demonstrated that TCR ligation results in the transactivation of CXCR4 defined as phosphorylation of CXCR4 that results in the formation of TCR–CXCR4 complexes in the absence of its ligand CXCL12. The formation of these TCR–CXCR4 complexes activates a PREX1/Rac-1 pathway and enhances cytokine mRNA stability (12). Understanding the mechanisms by which the TCR transactivates and physically associates with CXCR4 to form a TCR–CXCR4 heterodimer could lead to the discovery of new ways to therapeutically modulate cytokine production and thus treat disease.

Ligand-induced receptor heterodimers have been discovered in multiple cell types and shown to play critical roles in cellular function (17, 18). Receptor heterodimers significantly expand the biological outcomes arising from ligation of a particular receptor by producing signaling outcomes distinct from either receptor alone (19). These receptor heterodimers permit the ligated receptor to access signal transduction machinery associated with the other receptor and thus couple to additional signaling pathways (20–22). In various cell types, receptor tyrosine kinases (RTKs) have been shown to be able to transactivate CXCR4 and thus use CXCR4 to couple to a variety of CXCR4-dependent signaling pathways (12, 23, 24). For example, stem cell factor signaling through c-Kit results in the transactivation of CXCR4 and thereby regulates cardiac stem cell migration into infarcted cardiac tissue (25). Moreover, insulin-like growth factor-1 receptor (IGF-1R) transactivation of CXCR4 is required for IGF-1–mediated metastasis in breast cancer (23).

Despite progress in understanding the molecular mechanisms of RTK cross-regulation of CXCR4, little is currently understood about how an antigen-recognition receptor such as the TCR is able to transactivate and form heterodimers with CXCR4. RTK transactivation of CXCR4 has been shown in several cases to be associated with serine phosphorylation of CXCR4, which stimulates downstream outcomes such as cell motility, tumorigenesis, MAPK signaling, β-arrestin–mediated signaling, and receptor desensitization (25–29). The CXCR4 cytoplasmic C-terminal "tail" domain contains multiple serines that can be phosphorylated. Several Ser/Thr kinases activated downstream of RTKs have been shown to be capable of phosphorylating CXCR4 at various sites, including PKC isoforms, PIM1, and G protein–coupled receptor kinases (GRKs) (25, 30). The seven GRK family members represent three distinct families: the GRK1 family (GRK1 and GRK7), the GRK2 family (GRK2 and GRK3), and the GRK4 family (GRK4, GRK5, and GRK6). The GRK families share the N-terminal, catalytic, and RH domains; however, the GRK2 family has an additional pleckstrin homology domain that can bind to Gβγ (31). T cells have been shown to express high levels of GRK2 and GRK3, and TCR stimulation further increases their expression (32). Yet, until now, no role for a GRK in the mediation of TCR-induced cytokine production, CXCR4 transactivation, or TCR–CXCR4 complex formation has been described.

Recent studies from our laboratory demonstrated that CXCR4 is required for the TCR to stimulate a PREX1/Rac-1 signaling pathway that is required for stabilization of the cytokine mRNA transcripts (12). However, the molecular mechanism responsible for the coupling of these receptors to PREX1 following TCR stimulation was not known. In other cell types, the Rac–GEF PREX1 can be regulated downstream of GPCRs via the G protein subunits Gβγ and via the generation of PIP$_3$ by PI3Kγ, which results in the plasma membrane recruitment and activation of PREX1 (24, 33). PI3Kγ is composed of the catalytic subunit p110-γ and either of the p101 or p85 regulatory subunits, and it can be activated via Gβγ signaling downstream of GPCRs (34). PI3Kδ has previously been linked to TCR signaling, T cell development, and immune function (35, 36); however, the role of PI3Kγ downstream of TCR stimulation has not been fully characterized.

Here, we identify a previously unknown function of GRK2 as a target of TCR-stimulated tyrosine kinases. We also show that GRK2 is required for the TCR-mediated transactivation of CXCR4, mediating phosphorylation of the CXCR4 residue Ser-339, which is required for TCR–CXCR4 complex formation. Consistent with these results, we additionally show that either depletion or inhibition of GRK2 significantly impaired the ability of T cells to produce high levels of IL-2 and IL-10 cytokines. Furthermore, PREX1 localization was inhibited using the PI3Kγ inhibitor IPI-549, and either inhibition or depletion of PI3Kγ significantly reduced TCR-mediated cytokine production. Together, these results significantly expand understanding of the molecular mechanisms responsible for cross-regulation of CXCR4 and the TCR in T cells.

Results

Cytoplasmic C-terminal tail domain of CXCR4 is required for the formation of TCR–CXCR4 complexes in response to TCR/CD3 stimulation

We previously reported that the association of TCR with CXCR4 in response to ligation of the TCR is required for activation of a cytokine mRNA stabilization pathway that leads to robust production of IL-2 and IL-10 (12). To begin to address the molecular mechanisms responsible for receptor transactivation in this pathway, we determined the role of the cytoplasmic C-terminal tail portion of CXCR4, which contains several motifs known to regulate signaling (26, 30, 37, 38). Fluorescence resonance energy transfer (FRET) (10–12) was used to measure TCR–CXCR4 complex formation before and after TCR ligation and stimulation via cross-linked CD3 mAb. FRET occurs when the CFP-tagged molecule comes within 10 nm of the YFP-tagged molecule resulting in donation of energy upon exposure to 433 nm of light (Fig. 1A). Jurkat T cells were transiently transfected with plasmids encoding CD3-ζ–CFP and either WT CXCR4 (WT–CXCR4–YFP) or Δ322-CXCR4 (Δ322–CXCR4–YFP), which has the C-terminal tail region truncated at amino acid residue 322 (Fig. 1B) (39). WT–CXCR4–YFP and Δ322–CXCR4–YFP were expressed on the cell surface at similar levels, resulting in an ~2-fold increase in CXCR4 cell-surface levels in cells expressing these constructs as compared with cells transfected with the control vector (Fig. 1, C and D). As we showed previously (12), in cells expressing WT–CXCR4–YFP, 20 min of TCR/CD3 stimulation resulted

SASBMB

J. Biol. Chem. (2018) 293(36) 14022–14039 **14023**

GRK2 is required for TCR-induced TCR–CXCR4 complex formation
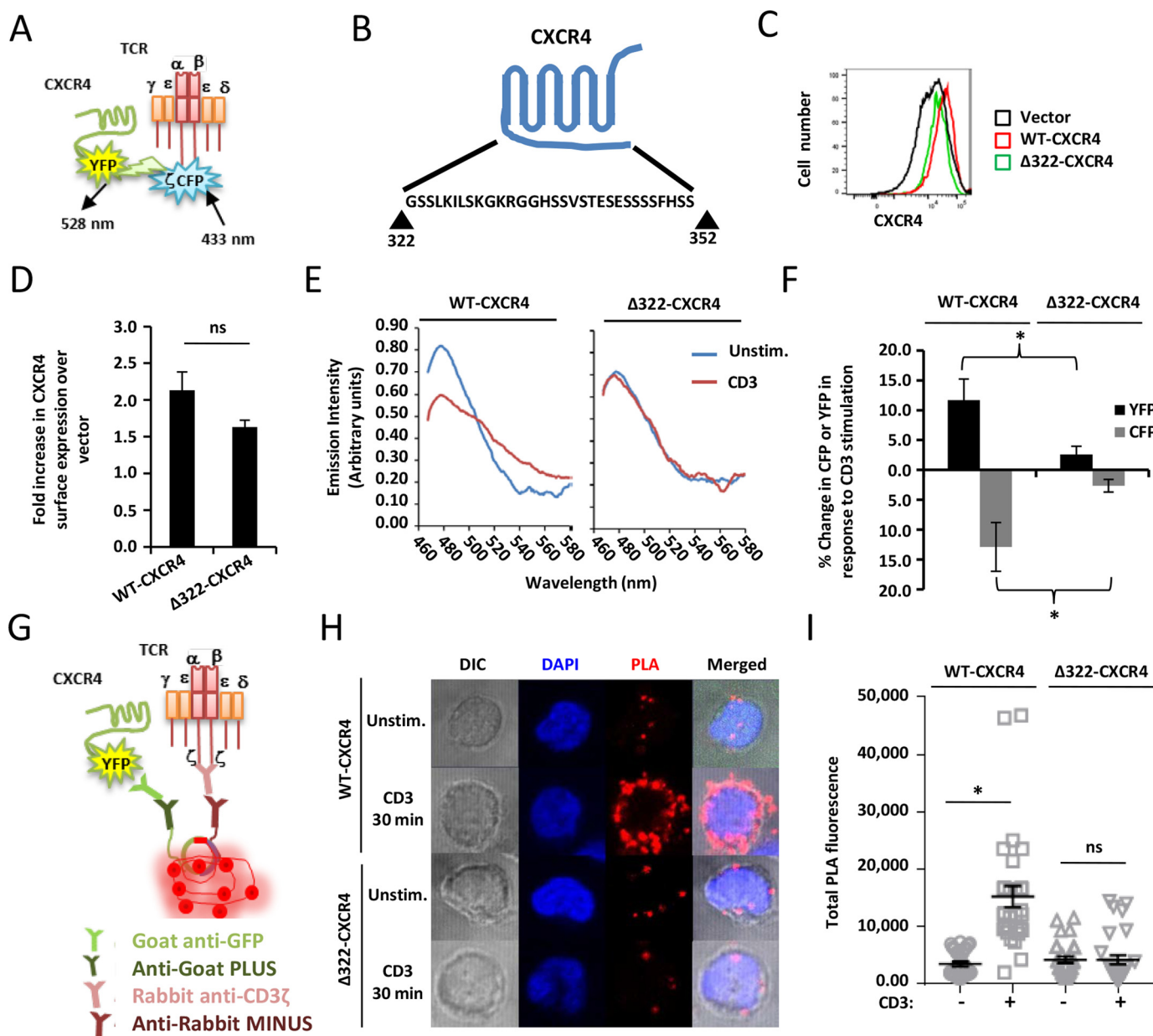
Figure 1. Cytoplasmic C-terminal tail region of CXCR4 is required for the formation of TCR–CXCR4 complexes in response to TCR/CD3 stimulation. *A,* schematic diagram of the FRET method used to detect the TCR signaling-induced close proximity of fluorescent fusion proteins of CXCR4 and CD3-ζ in *C–F. B,* diagram of CXCR4 indicating the amino acid residues eliminated by truncation of the cytoplasmic C-terminal tail at amino acid residue 322. *C–F,* Jurkat T cells were transiently transfected with either WT–CXCR4–YFP or Δ322–CXCR4–YFP and CD3ζ–CFP. *C,* representative histograms displaying CXCR4 cell-surface expression on the transfected cells as analyzed by flow cytometry. *D,* summary of three independent experiments performed as in *C;* the *bars* depict the mean fold-increase of CXCR4 cell-surface expression on the cells transfected with the indicated CXCR4 construct as compared with vector-transfected cells, ± S.E. (*E*). The transfected cells were stimulated with 1 μg/ml OKT3 and cross-linked with 0.1 mg/ml goat anti-mouse immunoglobulin G (IgG) for 20 min. Spectra of the same cells were analyzed for FRET before and after TCR/CD3 stimulation. Representative spectra from a single experiment are shown. *F,* summary of three independent experiments performed as in *E;* each *bar* represents the TCR/CD3 stimulation-induced percent change in CFP and YFP emission ± S.E.; *, significantly different from WT–CXCR4–YFP-expressing cells analyzed the same day (*p* < 0.05). *G,* schematic diagram of the PLA method used to detect the TCR-induced close proximity of CXCR4–YFP and endogenous CD3ζ in *H* and *I. H* and *I,* Jurkat T cells were transiently transfected with either WT–CXCR4–YFP or Δ322–CXCR4–YFP and then stimulated where indicated for 30 min with plate-bound CD3 mAb. *H,* representative images from a single experiment (original magnification ×100); *red* denotes PLA fluorescence that indicates receptor proximity; *DAPI* stains indicate cell nuclei; differential interference contrast (*DIC*) shows white light images of the cells. *I,* summary of three independent experiments performed as in *H;* 30 total cells were imaged and quantified per condition, and the mean total fluorescence ± S.E. is indicated; *, significantly increased in PLA fluorescence in stimulated cells as compared with unstimulated cells (*p* < 0.05). *ns,* not statistically significant.

in increased fluorescence in the YFP emission region (525–550 nm) and a corresponding decreased fluorescence in the CFP emission region (460–500 nm), indicating the formation of TCR–CXCR4 complexes detectable by FRET (Fig. 1*E*). In contrast, CD3-ζ–CFP failed to donate energy to Δ322–CXCR4–

YFP, indicating that the CXCR4 cytoplasmic tail is required for TCR–CXCR4 complex formation (Fig. 1*E*). Fig. 1*F* summarizes the results from multiple experiments performed as in Fig. 1*E*. To confirm these results, we assayed TCR–CXCR4 complex formation via proximity ligation assay (PLA), performed as
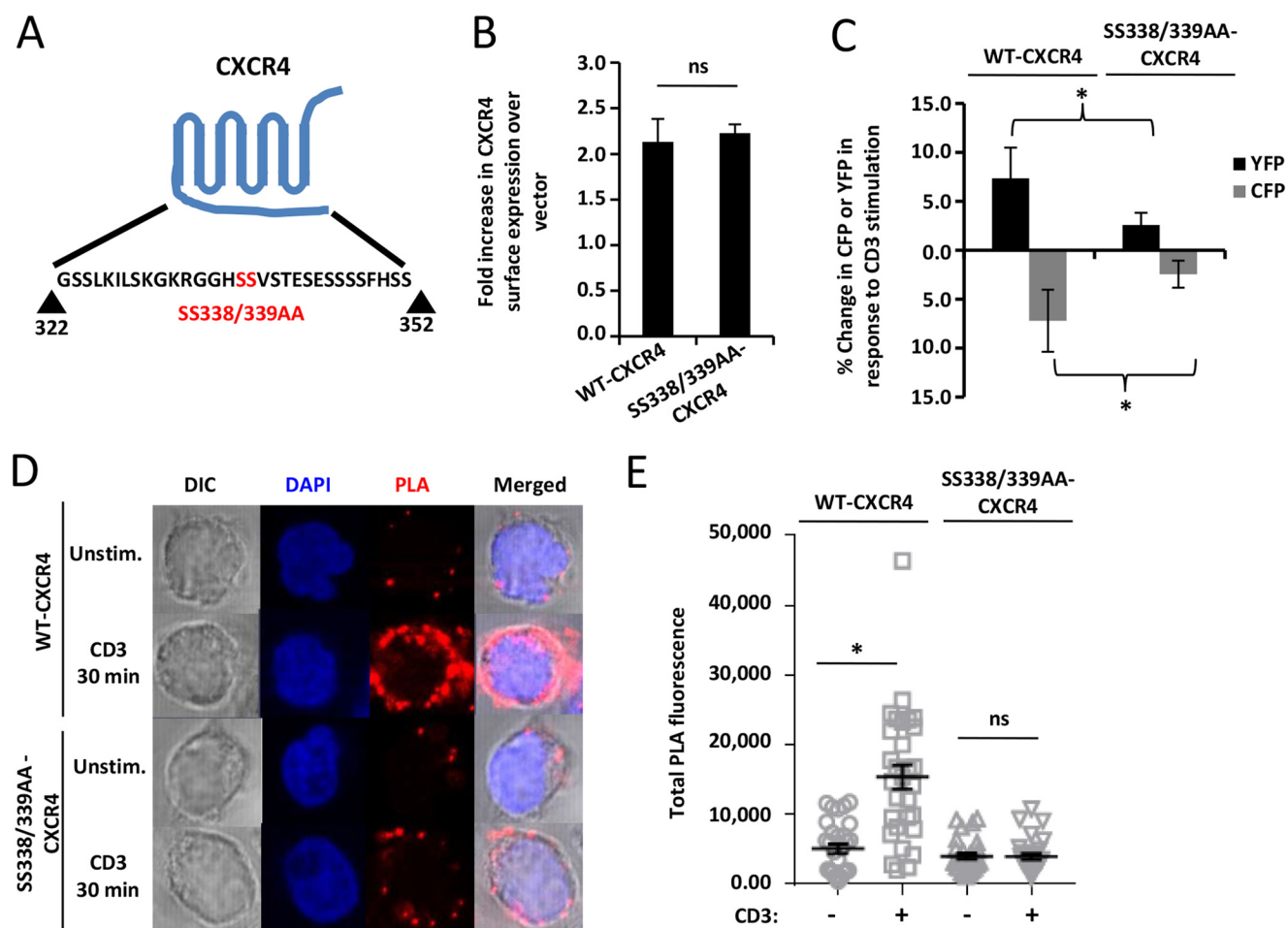
Figure 2. Serine residues 338 and 339 in the CXCR4 cytoplasmic tail are required for the formation of TCR–CXCR4 complexes in response to TCR/CD3 stimulation. *A,* schematic diagram of CXCR4 indicating the serine residues 338 and 339 that were mutated to alanine in SS338/339AA–CXCR4. *B and C,* Jurkat T cells were transiently transfected with CD3ζ–CFP and either WT–CXCR4–YFP or SS338/339AA–CXCR4–YFP as in Fig. 1, *B–F*. *B,* cell-surface expression of the indicated CXCR4 constructs, assayed by flow cytometry as in Fig. 1, *C and D*. *Bars* denote mean fold-increase in cell-surface expression of CXCR4 ± S.E.; $n = 3$. *C,* FRET analysis was performed as in Fig. 1, *C–F*. A summary of three independent experiments is shown; each *bar* represents the mean percent change ± S.E. in CFP or YFP emission, respectively, in response to CD3 stimulation; *, significantly different from responses of cells expressing WT–CXCR4–YFP analyzed the same day ($p > 0.05$). *D and E,* PLA analysis was performed as in Fig. 1, *H and I*. *D,* representative images acquired the same day. *E,* summary of images was acquired in three independent experiments for a total of 30 cells per condition, and the mean total fluorescence ± S.E. is indicated; *, significantly increased PLA fluorescence is stimulated as compared with unstimulated cells ($p < 0.05$). *DIC,* differential interference contrast. *ns,* not statistically significant.

described previously (12). PLA detects close interactions between two proteins via specific primary antibodies that bind to each protein and oligonucleotide-coupled secondary antibodies which, if in close proximity (<40 nm), result in oligonucleotide ligation, amplification, and visualization via *in situ* hybridization and confocal microscopy (Fig. 1*G*). Following a 30-min stimulation of the TCRs of Jurkat T cells transfected with either WT–CXCR4–YFP or Δ322–CXCR4–YFP, the cells were fixed and stained with primary antibodies directed against endogenous CD3-ζ and YFP. TCR–CXCR4 complex formation was then assessed via PLA. Low levels of TCR–CXCR4 complex formation were detected in the absence of TCR stimulation, as shown by the minimal PLA (*red*) fluorescence in unstimulated cells (Fig. 1*H*). PLA fluorescence significantly increased following TCR ligation of WT–CXCR4-expressing cells, consistent with TCR–CXCR4 complexes formed in response to TCR/CD3 stimulation (Fig. 1*H*). In contrast, cells expressing Δ322–CXCR4 failed to significantly increase PLA fluorescence upon T cell activation (Fig. 1*H*). Fig. 1*I* summarizes the results from multiple PLA experiments. Together, the results in Fig. 1 indi-

cate that the cytoplasmic carboxyl tail of CXCR4 is required for the formation of TCR–CXCR4 complexes in response to TCR/CD3-induced signaling.

Serine residues 338 and 339 in the CXCR4 cytoplasmic tail are required for the formation of TCR–CXCR4 complexes in response to TCR/CD3 stimulation

We previously showed that CXCR4 is phosphorylated on Ser-339 in response to TCR stimulation (12). To determine whether this phosphorylation is involved in mediating TCR–CXCR4 complex formation, we used a CXCR4 mutant (SS338/339AA–CXCR4–YFP) that has serine residues 338 and 339 mutated to alanine to eliminate their potential role as phosphorylation sites (Fig. 2*A*). SS338/339AA–CXCR4–YFP and WT–CXCR4–YFP constructs were expressed on the cell surface at similar levels (Fig. 2*B*). Interestingly, upon T cell activation, CD3-ζ–CFP failed to complex with and donate energy to SS338/339AA–CXCR4–YFP at levels comparable with WT–CXCR4–YFP via FRET analysis (Fig. 2*C*). Similarly, PLA analysis detected no significant complex formation of CD3-ζ

with SS338/339AA–CXCR4 upon ligation of TCR/CD3, compared with cells expressing WT–CXCR4 (Fig. 2, *D* and *E*). Together, these results indicate a critical role for CXCR4 Ser-338 and Ser-339 in the mechanism by which T cell activation leads to TCR–CXCR4 complex formation.

The GRK2-specific inhibitor, paroxetine, impairs TCR/CD3-stimulated CXCR4 Ser-339 phosphorylation, TCR–CXCR4 complex formation, and downstream IL-2 production

We next sought to identify the kinase responsible for phosphorylating CXCR4 Ser-339 in response to TCR stimulation. G protein–coupled receptor kinases (GRKs) are Ser/Thr kinases that are capable of phosphorylating several residues of the CXCR4 tail domain following CXCR4 stimulation by its chemokine ligand, CXCL12 (26, 30, 40). A previous study showed that GRK2 constitutively associates with the TCR subunit CD3-ε in T cells (41), suggesting a role for GRK2 in TCR signaling. To determine whether GRK2 is required for TCR-mediated TCR–CXCR4 complex formation, we first inhibited GRK2 kinase activity via the specific inhibitor, paroxetine (42, 43). Jurkat T cells were transfected as in Fig. 1, *C–F*, pretreated with 0.1 μM paroxetine, and then assayed for TCR–CXCR4 complex formation via FRET in response to TCR/CD3 stimulation. Cells pretreated with paroxetine displayed similar levels of CXCR4 cell-surface expression as compared with vehicle-treated cells (Fig. 3*A*). Interestingly, TCR/CD3-stimulated TCR–CXCR4 complex formation as detected by FRET was significantly inhibited by paroxetine treatment as compared with vehicle-treated control cells (Fig. 3*B*). Moreover, paroxetine treatment significantly inhibited the increased phosphorylation of CXCR4 Ser-339 seen in response to TCR/CD3 stimulation (Fig. 3, *C* and *D*), indicating that GRK2 activity is required for both the TCR/CD3 signaling-induced transactivation of CXCR4 and for TCR–CXCR4 complex formation.

We also assessed the role of GRK2 activity in the mechanism by which TCR signaling induces robust cytokine secretion, because this was previously shown to be a downstream outcome of TCR–CXCR4 complex formation in T cells (12). Normal human T cells were purified from the peripheral blood of healthy donors (PBMC T cells), pretreated with either 3 μM paroxetine or vehicle, and then assayed for cytokine secretion following activation with CD3 and CD28. Treatment of PBMC T cells with this concentration of paroxetine did not increase cell death during this assay as determined by annexin V staining (Fig. 3, *E* and *F*) or alter CXCR4 cell-surface expression (Fig. 3*G*). We assayed IL-2, IFNγ, and IL-10 secretion in response to TCR ligation. Fig. 3, *H* and *I*, shows the cytokine secretion results of each individual blood donor as a *colored line*, and the *black lines* show the average results of all blood donors ± S.E. Fig. 3*H* demonstrates, as expected, that anti-CD3 and anti-CD28 stimulation is required for detectable cytokine production by the PBMC T cells. Importantly, the results in Fig. 3*I* show that IL-2 cytokine production by TCR/CD3 + CD28–stimulated human T cells is significantly decreased by paroxetine pretreatment, consistent with paroxetine inhibiting the upstream GRK2-dependent process of TCR-induced TCR–CXCR4 complex formation. IL-10 production trended downward with paroxetine treatment (Fig. 3*I*). Although not statisti-

cally significant, this downward trend is consistent with the expected effects of blocking TCR-induced TCR–CXCR4 formation on IL-10 production (12). As shown previously (12), IFN-γ was not significantly inhibited upon disruption of TCR–CXCR4 complex formation (Fig. 3*I*). Together, the results in Fig. 3 indicate that treatment of T cells with the GRK2-specific inhibitor, paroxetine, inhibits TCR-induced TCR–CXCR4 complex formation, phosphorylation of CXCR4 Ser-339, and also downstream IL-2 production previously shown to be dependent on TCR–CXCR4 complex formation.

siRNA-mediated depletion of GRK2 significantly inhibits TCR/CD3-stimulated phosphorylation of CXCR4 Ser-339 and TCR–CXCR4 complex formation

To confirm the role of GRK2 in T cell signaling, we depleted GRK2 in Jurkat T cells via transfection of GRK2-specific siRNA, and we determined the effects on TCR-induced TCR–CXCR4 complex formation. Compared with cells transfected with control siRNA, cells transfected with either GRK2 siRNA #1 or GRK2 siRNA #2 significantly depleted GRK2 protein levels by ~50% (Fig. 4, *A* and *F*) while having no significant effects on CXCR4 cell-surface levels (Fig. 4, *B* and *G*). FRET experiments performed as in Fig. 1, *E* and *F,* revealed that TCR/CD3-stimulated TCR–CXCR4 complex formation was significantly inhibited by depletion of GRK2 (Fig. 4, *C* and *H*). Depletion of GRK2 also significantly inhibited the phosphorylation of CXCR4 Ser-339 in response to TCR/CD3 stimulation (Fig. 4, *D* and *E*). Together, these experiments indicate that GRK2 is required for TCR–CXCR4 complex formation as well as phosphorylation of CXCR4 Ser-339 in response to T cell activation.

GRK2 is required for TCR/CD3-induced IL-2 and IL-10 production by normal human T cells purified from peripheral blood

Because TCR–CXCR4 complex formation is known to be required for high IL-2 and IL-10 production following ligation of the TCR (12), we also examined the effect of GRK2 depletion on cytokine secretion. Human PBMC T cells were transiently transfected with either GRK2 siRNA #1 or GRK2 siRNA #2, which reduced GRK2 protein expression by ~50% (Fig. 5, *A* and *E*) while having no detectable effect on cellular apoptosis (Fig. 4, *B* and *F*) or CXCR4 cell-surface expression (Fig. 5, *C* and *G*). Importantly, TCR/CD3-stimulated production of both IL-2 and IL-10 was significantly inhibited in GRK2-deficient human T cells transfected with either GRK2 siRNA #1 or #2 (Fig. 5, *D* and *H*). IFN-γ production was not significantly altered by depletion of GRK2 (Fig. 5, *D* and *H*), consistent with our previous report that production of this cytokine is less impacted by TCR–CXCR4 formation than IL-2 and IL-10 (12). Altogether, the results in Figs. 3–5 indicate that GRK2 is required for the TCR/CD3 ligation-induced signaling pathway that results in the phosphorylation of CXCR4 at Ser-339, and this event is required for TCR–CXCR4 complex formation necessary for the robust downstream production of IL-2 and IL-10 cytokines by stimulated T cells.
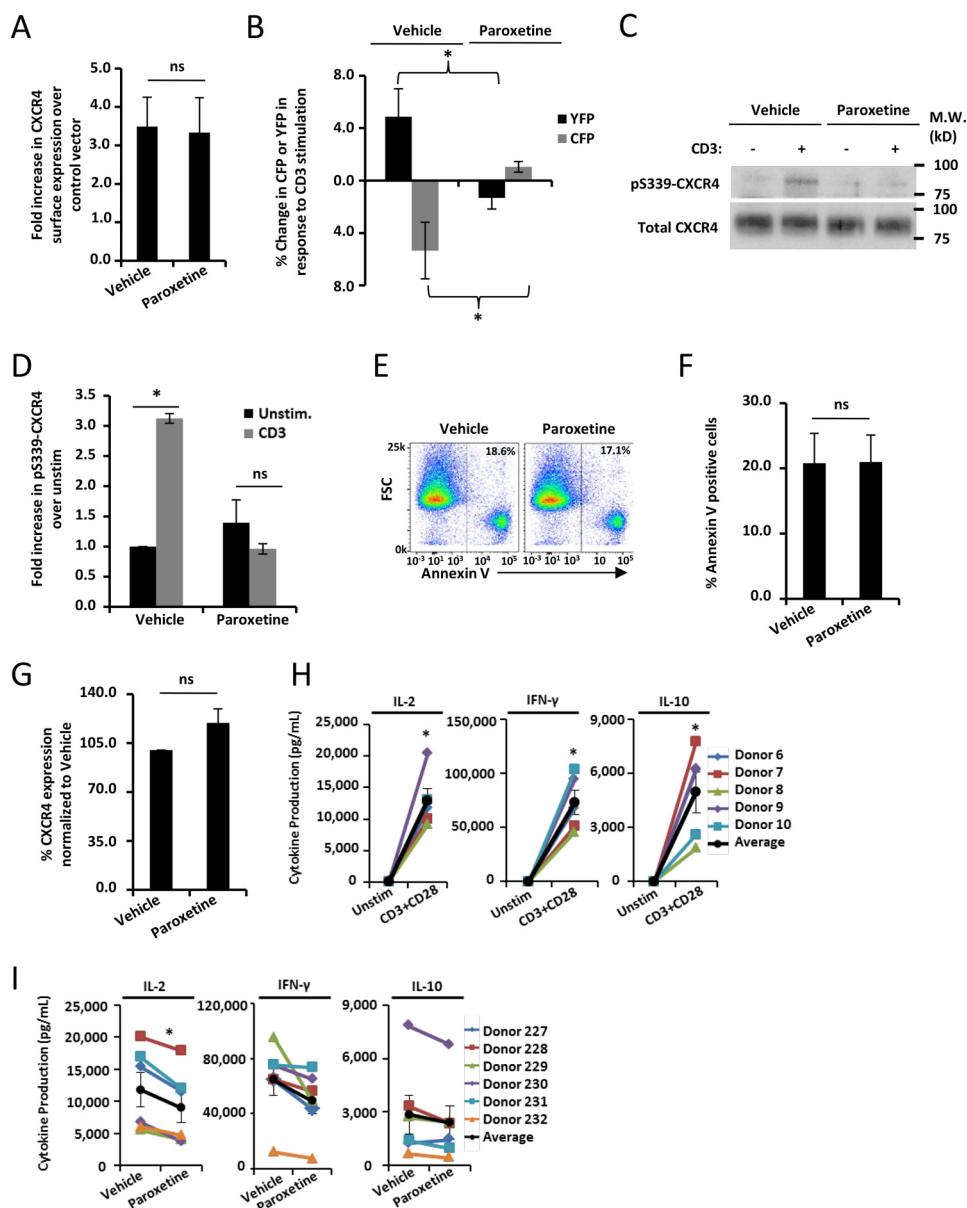
Figure 3. GRK2-specific inhibitor, paroxetine, impairs TCR/CD3-stimulated CXCR4 Ser-339 phosphorylation, TCR–CXCR4 complex formation, and IL-2 production. *A* and *B*, Jurkat T cells were transiently transfected as in Fig. 1, *C–F*, and pretreated with 0.1 μM paroxetine for 1 h. *A*, CXCR4 cell-surface expression was measured as in Fig. 1, *C and D* ($n = 3$). *B*, summary of TCR/CD3-induced TCR–CXCR4 complex formation assayed by three independent FRET experiments performed as in Fig. 1, *E and F*; *, significantly different from the results of vehicle-treated cells ($p < 0.05$). *C* and *D*, Jurkat T cells were transiently transfected with WT–CXCR4–YFP and cultured for 16 h. Cells were pretreated with 0.1 μM paroxetine or vehicle for 1 h followed by stimulation with 1 μg/ml biotinylated CD3 mAb cross-linked with 1 mg/ml avidin for 5 min. Cells were then lysed, and WT–CXCR4–YFP was immunoprecipitated by anti-GFP and analyzed by SDS-PAGE and immunoblotting for pSer-339–CXCR4 and total CXCR4. *D*, summary of densitometry of three experiments performed as in *C*; *bars* denote the mean fold-increase in pSer-339–CXCR4 in response to TCR/CD3 stimulation as compared with unstimulated cells ± S.E. ($p < 0.05$). *E–I*, T cells from normal healthy humans (PBMC T cells) were purified from peripheral blood and then pretreated with vehicle or 3 μM paroxetine for 1 h prior to stimulation. PBMC T cells were then stimulated with 1 μg/ml plate-bound OKT3 and soluble CD28 for 24 h. *E* and *F*, paroxetine pretreatment failed to significantly increase T cell apoptosis as assayed via staining with APC-conjugated annexin-V and flow cytometry; *E*, representative results; *F*, summary of apoptosis assays performed as in *E* for four different T cell donors, mean % of annexin-V–positive cells ± S.E. *G*, CXCR4 cell-surface expression on PBMC T cells after 1 h of pretreatment with 3 μM paroxetine or vehicle-treated cells (±S.E.; $n = 4$ individual blood donors). *H* and *I*, PBMC T cells were unstimulated or stimulated with CD3 + CD28 mAb for 24 h. Where indicated, PBMC T cells were pretreated with paroxetine for 1 h. Supernatants were harvested and analyzed for cytokine production by ELISA. Results are from six different T cell donors; *black lines* denote the average results of all donors tested ± S.E.; *, significantly different from vehicle-pretreated cells; $p < 0.05$. *ns,* not statistically significant.

TCR/CD3-stimulated Src family and ZAP-70 tyrosine kinases are required for TCR–CXCR4 complex formation

To explore the molecular mechanisms by which TCR signaling leads to GRK2 activation, we sought to identify TCR-induced kinases required for TCR–CXCR4 complex formation. Previous studies have shown that Src kinases can activate or enhance GRK2 activity (44). TCR signaling proceeds via the Src-family tyrosine kinases Lck and Fyn (43). Therefore, we tested whether TCR-stimulated Src family and ZAP-70 tyrosine kinases are required for the GRK2-dependent events of CXCR4 Ser-339 phosphorylation and TCR–CXCR4 complex formation. PP2 inhibition of Src kinases significantly decreased
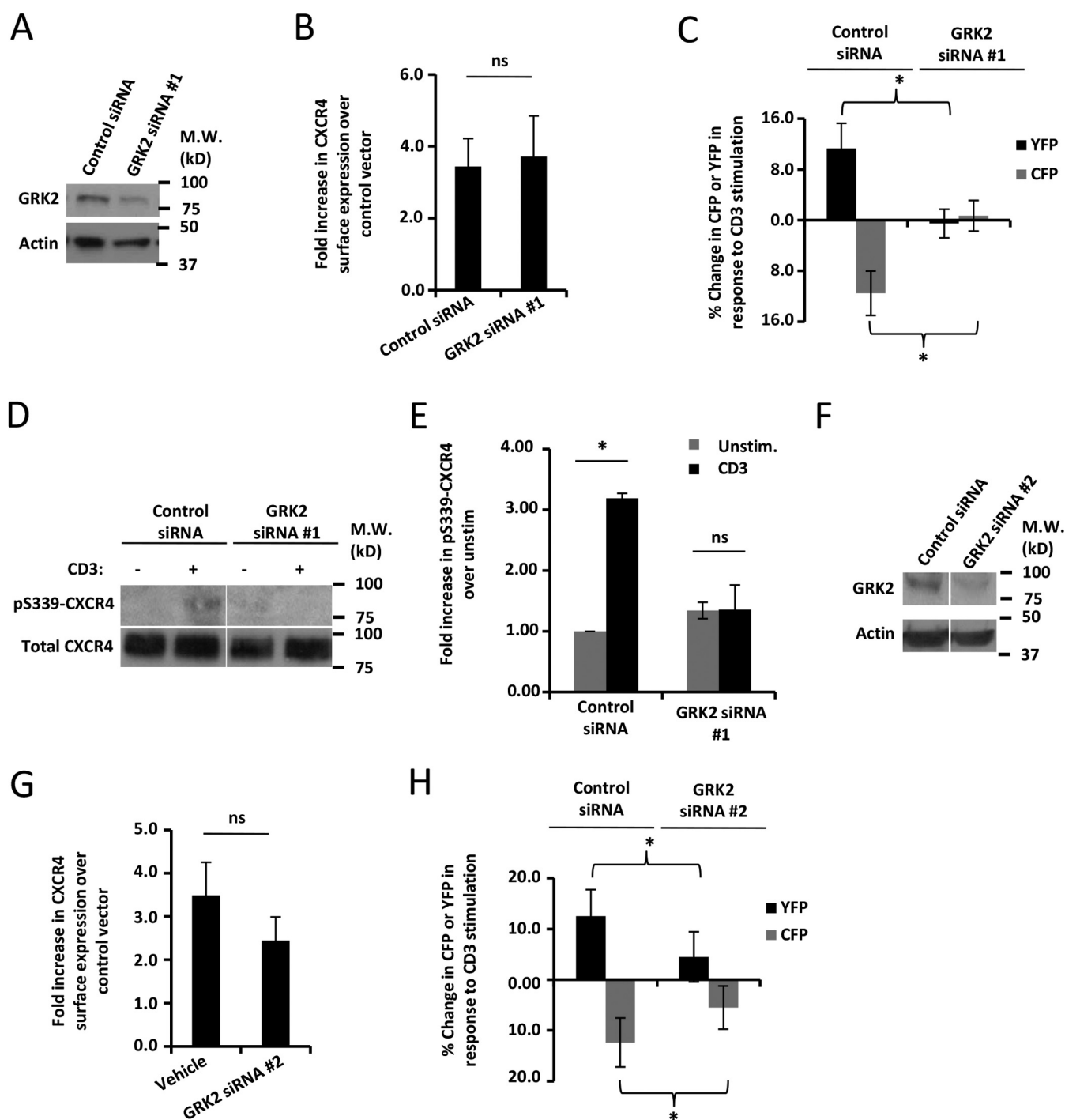
Figure 4. siRNA-mediated depletion of GRK2 significantly inhibits TCR/CD3-stimulated phosphorylation of CXCR4 Ser-399 and TCR–CXCR4 complex formation. *A–H*, Jurkat T cells were transiently transfected for FRET assays as in Fig. 1, *C–F*, except that the transfections also included either a control nontargeting siRNA pool, a pool of GRK2 siRNAs (*GRK2 siRNA #1*), or a single GRK2 siRNA (*GRK2 siRNA #2*). Following transfection, cells were cultured for 48 h to permit GRK2 depletion prior to analysis. *A* and *F*, representative immunoblots showing GRK2 depletion at 48 h. *B* and *G*, CXCR4 cell-surface expression at 48 h as determined by flow cytometry performed as in Fig. 1, *C and D*; ± S.E.; *n* = 3. *C* and *H*, summary of TCR/CD3-induced TCR–CXCR4 complex formation as determined by three independent FRET experiments performed as in Fig. 1, *E and F*; ± S.E.; *, significantly different from responses of control siRNA-transfected cells; *p* < 0.05. *D* and *E*, TCR/CD3-induced CXCR4 Ser-339 phosphorylation in GRK2-depleted cells was assayed as in Fig. 3, *C and D*; *D*, representative result; *E*, summary of densitometric quantitation of three independent experiments performed as in *D*; *bars* denote the mean fold-increase in pSer-339–CXCR4 in response to TCR/CD3 stimulation as compared with unstimulated cells analyzed the same day ± S.E.; *p* < 0.05. *ns*, not statistically significant.

the ability of TCR/CD3 stimulation to induce TCR–CXCR4 complex formation as assayed by either FRET or PLA (Fig. 6, *A*, *C*, and *D*). Additionally, we used piceatannol to inhibit ZAP-70, a tyrosine kinase that binds directly to the TCR and mediates TCR-induced signal transduction following Lck-dependent

TCR phosphorylation (45, 46). The results show that piceatannol pretreatment significantly decreased TCR-induced TCR–CXCR4 complex formation as assayed by either FRET or PLA (Fig. 6, *B, C,* and *D*). We further showed that pretreating cells with either PP2 or piceatannol significantly decreased TCR-
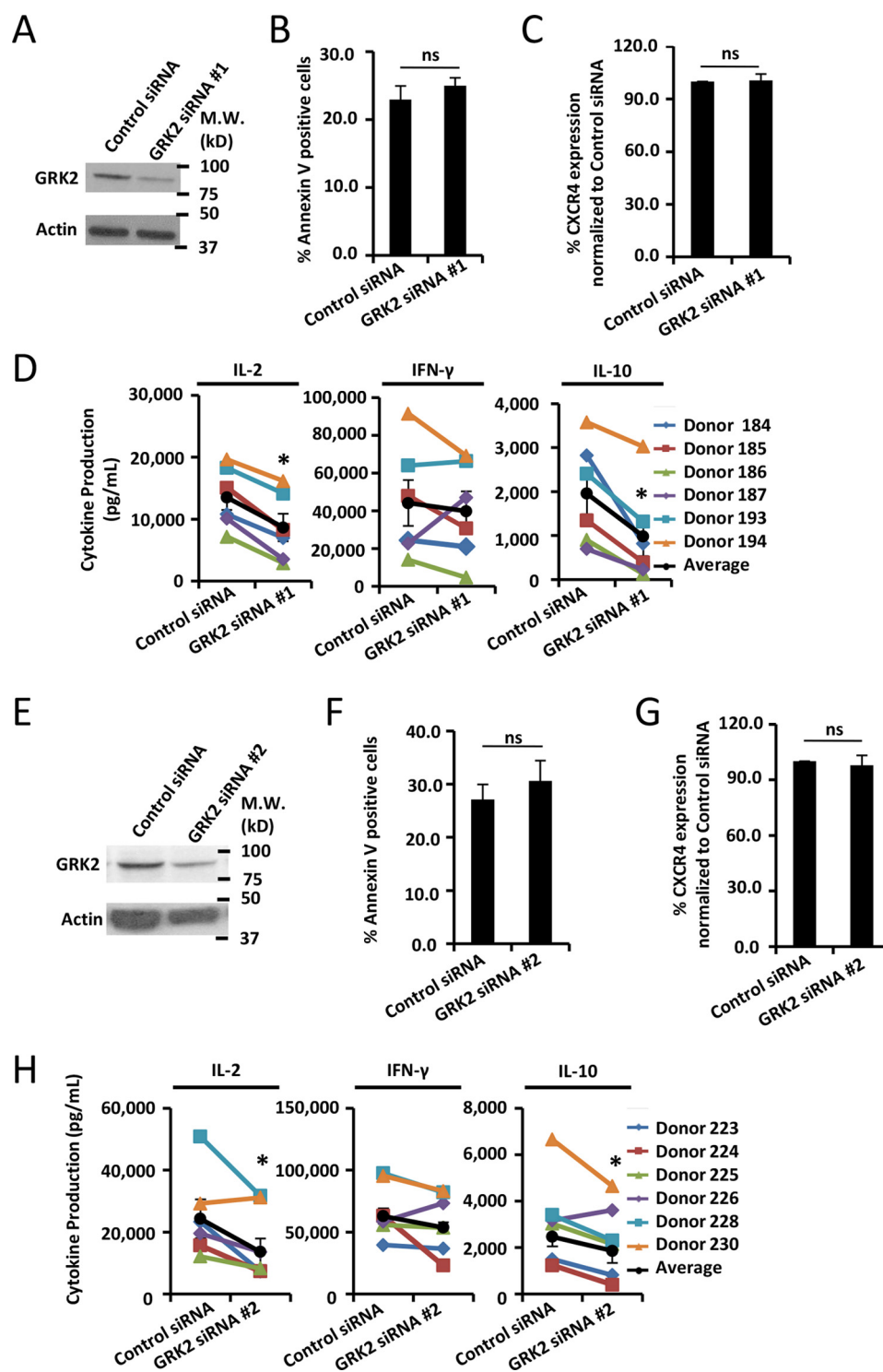
Figure 5. GRK2 is required for TCR/CD3-induced IL-2 and IL-10 production by normal human T cells purified from peripheral blood. *A–H,* PBMC T cells isolated from healthy human donors were transfected with either control nontargeting siRNA, GRK2 siRNA #1, or GRK2 siRNA #2 and then cultured for 48 h. *A* and *E,* representative immunoblots demonstrating GRK2 depletion at 48 h. *B* and *F,* after the 48-h incubation, the cells were stimulated with 1 mg/ml plate-bound OKT3 and soluble CD28 for 24 h, and then apoptosis was assayed via annexin-V staining as in Fig. 3, *E* and *F*. A summary of results from four different blood donors is shown for each GRK2 siRNA; *bars* denote the mean % of primary T cells staining positive for annexin-V $\pm$ S.E.; $n = 4$. *C* and *G,* CXCR4 cell-surface expression was measured via flow cytometry 48 h after depletion of GRK2 via siRNAs. *Bars* denote the mean percentage of CXCR4 expression as compared with control siRNA-transfected cells analyzed the same day $\pm$ S.E.; $n = 3$. *D* and *H,* human PBMC T cells were depleted of GRK2 as above and were then stimulated with CD3 + CD28 mAb for an additional 24 h as in Fig. 3*H*. Culture supernatants were then assayed for cytokines as in Fig. 3*H*. *, significantly different from control cells; $p < 0.05$. *ns,* not statistically significant.
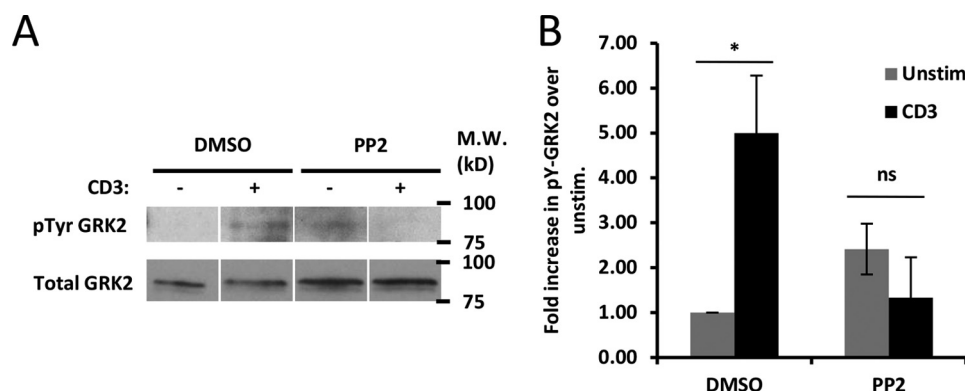
induced phosphorylation of CXCR4 Ser-339 (Fig. 6, *E* and *F*). Together, these results indicate that TCR-activated tyrosine kinases lead to activation of GRK2 and that GRK2 subsequently phosphorylates CXCR4 on Ser-339 to induce formation of the TCR–CXCR4 complexes responsible for the robust IL-2 and IL-10 cytokine secretion of TCR-activated T cells.
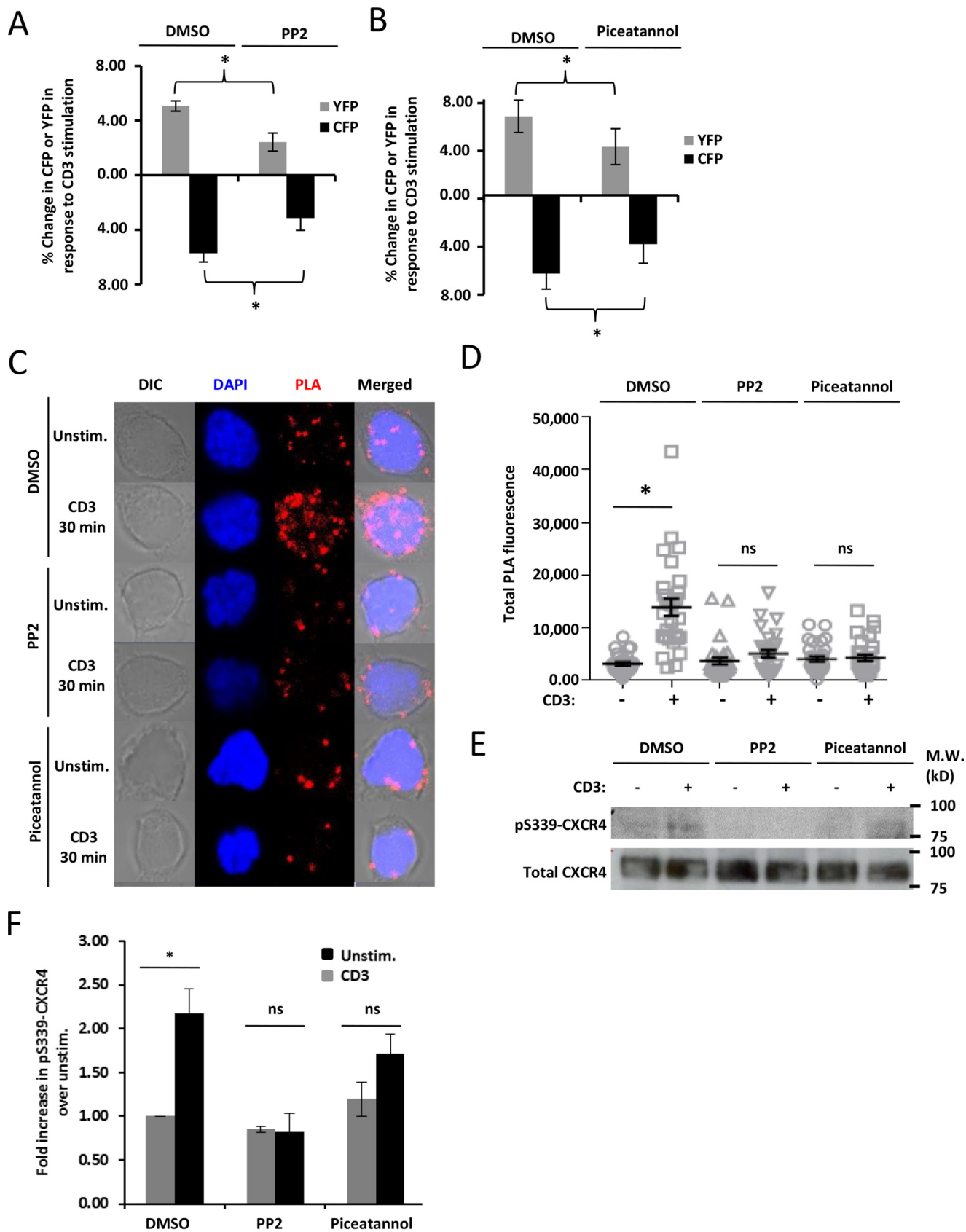
Figure 7. TCR/CD3 stimulation induces GRK2 tyrosine phosphorylation via a mechanism requiring an Src kinase. *A* and *B*, Jurkat T cells were pretreated with either DMSO or 1 μM PP2 for 30 min followed by 5 min of TCR/CD3 stimulation as in Fig. 3C. The cells were lysed, and GRK2 was immunoprecipitated and immunoblotted for phosphotyrosine using a pTyr-specific antibody. The same blot was stripped and re-probed for total GRK2 as a control. *A*, representative result; *B*, summary of three independent experiments performed as in *A* and quantified by densitometry; each *bar* denotes the mean fold-increase of pTyr GRK2 in TCR/CD3-stimulated cells as compared with unstimulated cells $\pm$ S.E.; *n* = 3; *, significantly different from unstimulated cells; *p* < 0.05. *ns,* not statistically significant.

TCR/CD3 stimulation induces tyrosine phosphorylation of GRK2 via a mechanism requiring a Src kinase

Next, we sought to determine whether GRK2 is tyrosine-phosphorylated in response to TCR/CD3 ligation. Src kinase-mediated phosphorylation of GRK2 has been shown to enhance GRK2 kinase activity downstream of EGFR activation (43, 44). Indeed, we found that CD3 mAb stimulation of Jurkat T cells for 5 min significantly increased the tyrosine phosphorylation of endogenous GRK2 by ~5-fold (Fig. 7, *A* and *B*). Consistent with this response being mediated by TCR/CD3-initiated signaling, this TCR/CD3-induced GRK2 tyrosine phosphorylation was abrogated by pretreating cells with the Src kinase inhibitor PP2 (Fig. 7, *A* and *B*) (47). Thus, the TCR/CD3 stimulation of T cells uses Src kinases to either directly or indirectly tyrosine-phosphorylate GRK2.

PREX1 plasma membrane localization depends on GRK2 and PI3Kγ

Because we previously demonstrated that activation of the PREX1/Rac-1 signaling pathway enhances the stability of IL-2, IFN-γ, and IL-10 transcripts (12), we sought to understand the role of GRK2-mediated transactivation of CXCR4 in PREX1 signaling. Activation of PREX1 can be initiated by its localization to the membrane from the cytoplasm (34, 48, 49); therefore, we assayed whether GRK2-mediated transactivation of CXCR4 mobilizes PREX1 to the membrane. Utilizing a PREX1–GFP fusion protein, Fig. 8A shows that CD3 stimulation induces the localization of PREX1–GFP to the plasma membrane in Jurkat T cells. Plasma membrane localization was measured using the fluorescence profile across the cell (Fig. 8A)

and calculated as a percent of PREX1 fluorescence at the cell membrane *versus* cytoplasm (Fig. 8B). Furthermore, inhibition of GRK2 with paroxetine led to a significant reduction in PREX1 membrane localization in response to TCR ligation (Fig. 8, *A* and *B*). PREX1 was previously shown to be recruited to the membrane downstream of GPCRs by PI3Kγ-generated PIP$_3$ (33, 48, 49). To assess the role of PI3Kγ in mediating PREX1 localization to the membrane in response to TCR stimulation, we used the PI3Kγ-specific inhibitor IPI-549. Interestingly, inhibition of PI3Kγ resulted in significantly impaired PREX1 membrane localization in response to TCR stimulation (Fig. 8, *C* and *D*). Together, the results in Fig. 8 indicate that GRK2 is required for PI3Kγ-dependent PREX1 membrane localization in response to TCR ligation.

PI3Kγ-specific inhibitor, IPI-549, impairs TCR/CD3-stimulated cytokine production by decreasing mRNA stability

To confirm the role of PI3Kγ in TCR-mediated cytokine production through PREX1 and mRNA stability (12), we treated PBMC T cells with the PI3Kγ-specific inhibitor IPI-549 and assayed cytokine production. Treatment of the PBMC T cells with 1 μM IPI-549 did not increase cell death as assayed by annexin V staining (Fig. 9A) or alter CXCR4 cell-surface expression (Fig. 9B). Nevertheless, inhibition of PI3Kγ with IPI-549 led to significant reductions in IL-2, IFN-γ, and IL-10 production (Fig. 9C). As a control to demonstrate IPI-549 does not inhibit IL-2 gene transcription, we utilized an IL-2 luciferase promoter construct. Inhibiting PI3Kγ did not significantly alter CD3 + CD28-induced transcription from the IL-2 promoter (Fig. 9D). In contrast, we found that inhibition of PI3Kγ with IPI-549 led to a decrease in the half-life of IL-2 and IFN-γ tran-

Figure 6. TCR/CD3-stimulated Src family and ZAP-70 tyrosine kinases are required for TCR–CXCR4 complex formation. *A* and *B*, Jurkat T cells were transiently transfected for FRET assays as in Fig. 1, *C–F*, except that where indicated cells were pretreated for 30 min with 10 μM PP2, 0.1 μM piceatannol, or DMSO (vehicle) prior to TCR/CD3 stimulation. TCR/CD3-stimulated TCR–CXCR4 complex formation was subsequently assayed by FRET as in Fig. 1, *E* and *F*. The results of three independent experiments are shown $\pm$ S.E.; *n* = 3; *, significantly different from vehicle (DMSO)-pretreated cells analyzed the same day; *p* < 0.05. *C* and *D*, Jurkat T cells were transiently transfected with WT–CXCR4–YFP and analyzed for TCR/CD3-stimulated TCR–CXCR4 complex formation by PLA as in Fig. 1, *G* and *H*, except that cells were pretreated with drugs or DMSO (vehicle) as in *A* and *B* prior to TCR/CD3 stimulation. *C*, representative images; *D*, summary of multiple images acquired in three independent experiments; the mean total cell fluorescence $\pm$ S.E. is shown; 30 total cells per condition were imaged and quantified; *, significantly increased PLA fluorescence was detected in stimulated cells as compared with unstimulated cells; *p* < 0.05. *E* and *F*, following pretreatment with the indicated inhibitor for 30 min, Jurkat T cells were stimulated via CD3 mAb, and pSer-339–CXCR4 was assayed as in Fig. 3, *C* and *D*. *E*, representative result; *F*, summary of three independent experiments performed as in *E* and quantified by densitometry $\pm$ S.E.; *, significantly different from vehicle (DMSO)-pretreated cells; *p* < 0.05. *DIC,* differential interference contrast. *ns,* not statistically significant.
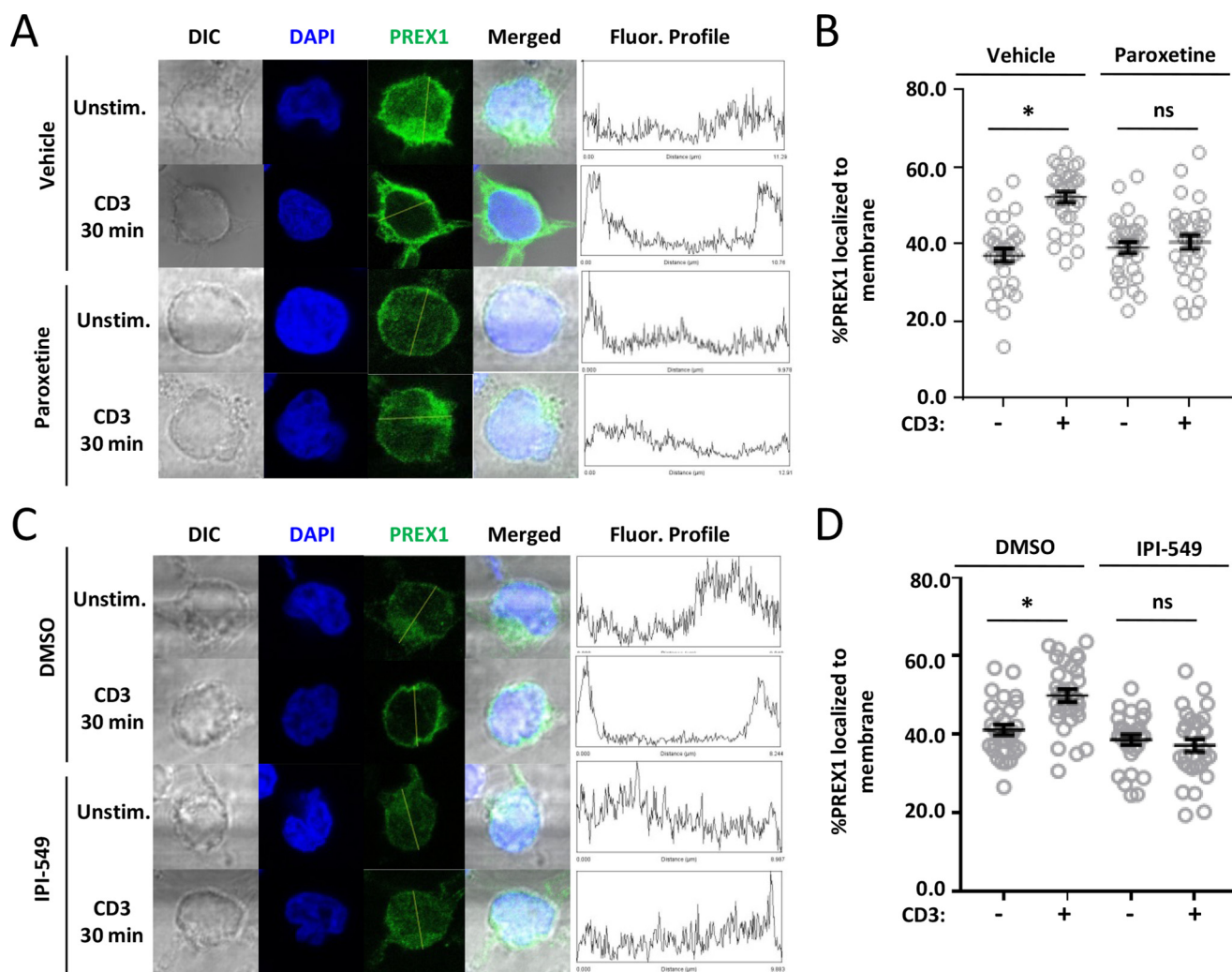
Figure 8. PREX1 membrane localization depends on GRK2-mediated transactivation of CXCR4 and PI3Kγ. *A–D,* Jurkat T cells were transiently transfected with eGFP-PREX1. Cells were fixed, permeabilized, mounted, and imaged. *A* and *C,* representative images and fluorescence profile for the indicated treatments. *B* and *D,* summary of multiple images acquired in three independent experiments; the mean percent PREX1 localized to membrane ± S.E. is shown; 30 total cells per condition were imaged and quantified; *, significantly increased membrane fluorescence was detected in stimulated cells as compared with unstimulated cells; $p < 0.05$. *DIC,* differential interference contrast. *ns,* not statistically significant.

scripts (Fig. 9, *E–H*). Fig. 9, *E* and *G,* shows representative mRNA decay curves of individual T cell donors for DMSO- and IPI-549–treated samples. Fig. 9, *F* and *H* summarizes the decreases in mRNA half-life for each individual donor tested. We were unable to measure the half-life of IL-10 transcripts in these donors' T cells because they were below the limit of detection for several time points. Together with the results in Fig. 8 indicating that PI3Kγ is required for TCR-mediated PREX1 membrane localization and our previous report that PREX1 mediates cytokine mRNA stabilization downstream of TCR–CXCR4 formation (12), the results in Fig. 9 indicate that PI3Kγ is required to couple TCR–CXCR4 to downstream PREX1-mediated cytokine mRNA stabilization that leads to enhanced cytokine production.
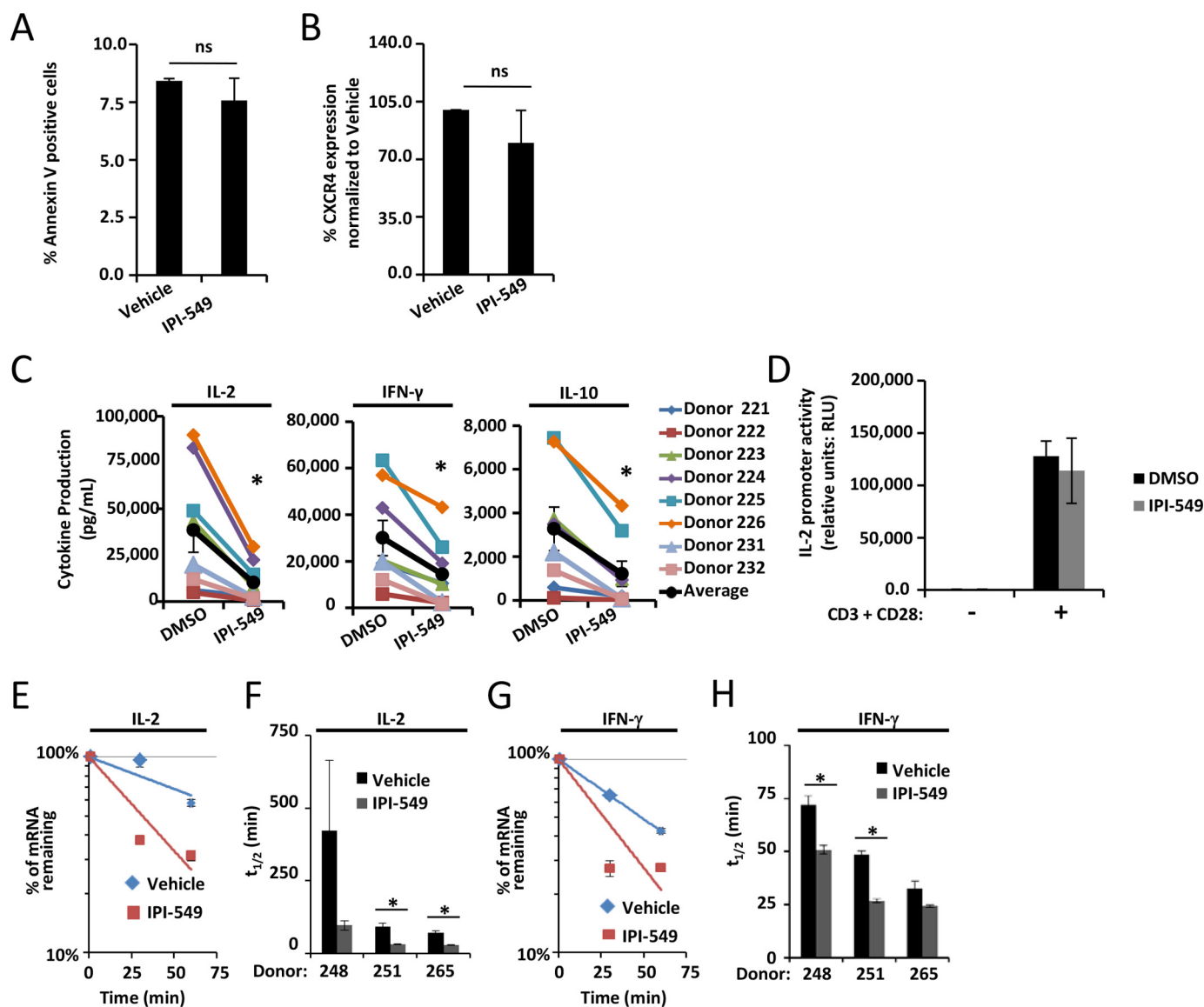
PI3Kγ is required for TCR/CD3-induced IL-2 and IL-10 production by normal human T cells purified from peripheral blood

To confirm the role of PI3Kγ in TCR/CD3-induced cytokine production, we depleted PI3Kγ via siRNA. Human PBMC T cells were transiently transfected with either PI3Kγ siRNA #1 or PI3Kγ siRNA #2, which reduced PI3Kγ protein expression by at least 50% (Fig. 10*A*) while having no detectable effect on cellular apoptosis (Fig. 10*B*) or CXCR4 cell-surface expression (Fig. 10*C*). Depletion of PI3Kγ with siRNA #1 led to a significant decrease in IL-2, IFN-γ, and IL-10 production (Fig. 10*D*). Depletion of PI3Kγ with siRNA #2 also led to a significant decrease in IL-2 (Fig. 10*E*). Although not significant, depletion of PI3Kγ with siRNA #2 resulted in a trend of decreased IL-10 production (Fig. 10*E*). IFN-γ production was not significantly altered upon depletion of PI3Kγ with siRNA #2 (Fig. 10*E*). These results are consistent with PI3Kγ being required for robust IL-2 and IL-10 production by TCR-stimulated primary human T cells.

GRK2 mediates TCR-induced transactivation of CXCR4 and TCR–CXCR4 complex formation required for PI3Kγ/PREX1 signaling and robust T cell cytokine secretion

Altogether, the results from this study led to the proposed model in Fig. 11; TCR/CD3 stimulation results in the activation
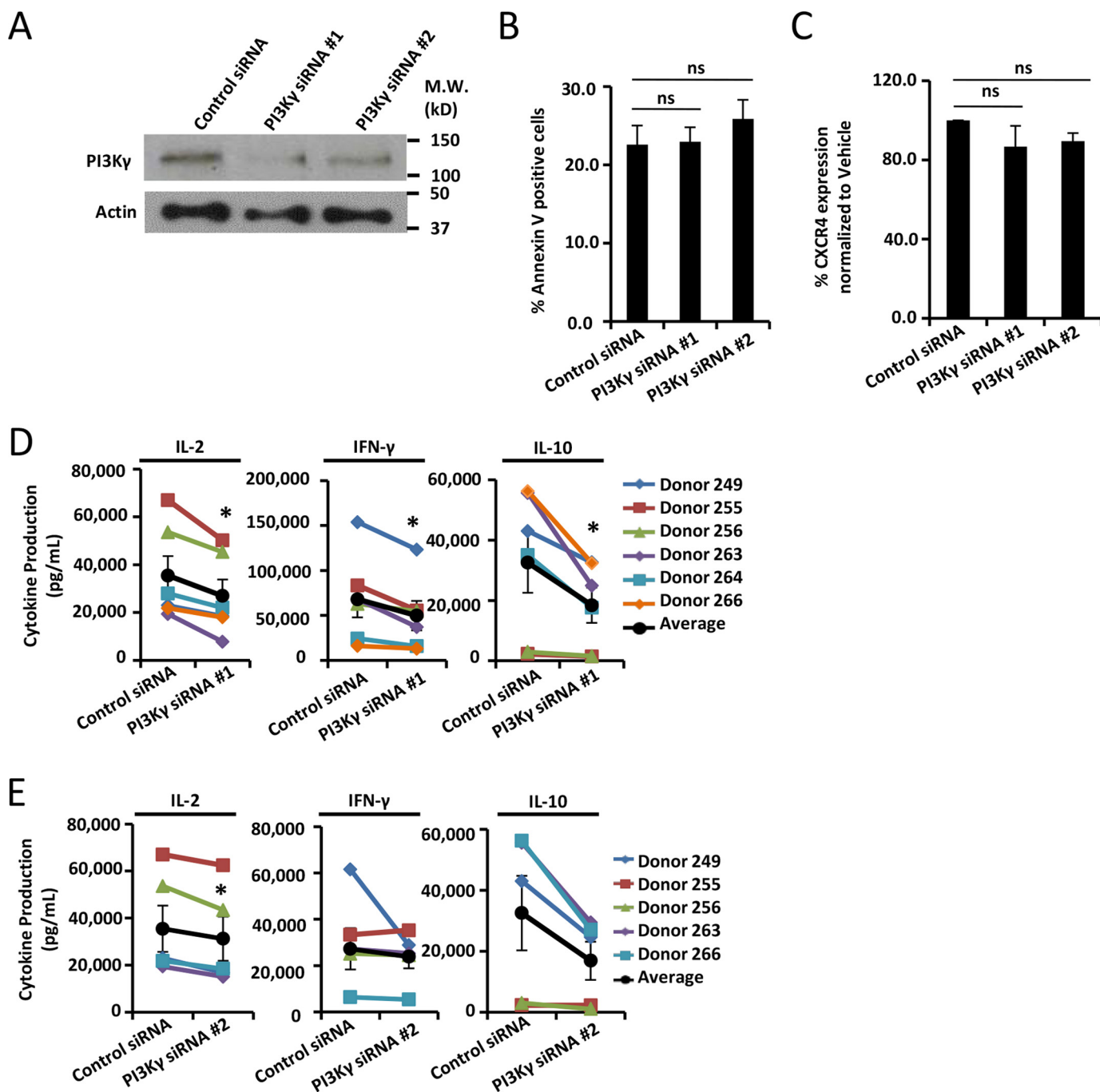
Figure 9. PI3Kγ is required for TCR/CD3-induced IL-2 and IL-10 production by normal human T cells purified from peripheral blood. *A–C,* PBMC T cells isolated from healthy human donors were cultured overnight and treated with DMSO or 1.0 μM IPI-549 for 1 h. *A,* after the 1-h treatment, the cells were stimulated with 1 mg/ml plate-bound OKT3 and soluble CD28 for 24 h, and apoptosis was assayed via annexin-V staining as in Fig. 3, *E* and *F*. Summary of results from four different blood donors are shown; *bars* denote the mean % of primary T cells staining positive for annexin-V ± S.E.; *n* = 4. *B,* CXCR4 cell-surface expression was measured via flow cytometry after treatment with DMSO or IPI-549. *Bars* denote the mean percentage of CXCR4 expression as compared with control DMSO-treated cells analyzed the same day ± S.E.; *n* = 4. *C,* human PBMC T cells were treated as above and were then stimulated with CD3 + CD28 mAb for 24 h as in Fig. 3*H*. Culture supernatants were assayed for cytokines as in Fig. 3*H*. *, significantly different from control cells; *p* < 0.05. *D,* Jurkat T cells were transiently transfected with an IL-2 promoter luciferase reporter construct, incubated for 16–18 h, treated with 1.0 μM IPI-549 for 1 h, stimulated with 1 mg/ml plate-bound OKT3 and soluble CD28 for 16 h, and then assayed for luciferase activity. Each *bar* denotes the mean relative light units (*RLU*) ± S.E., *n* = 3, *p* > 0.05. *E–H,* PBMC T cells were pretreated with IPI-549 for 1 h and then stimulated with 1 mg/ml plate-bound OKT3 and soluble CD28 5.5 h prior to addition of actinomycin D. mRNA levels of the indicated cytokine mRNA were assayed via qRT-PCR at the indicated times after addition of actinomycin D. *E* and *G,* representative mRNA decay curve for IL-2 mRNA (*E*) and IFN-γ (*G*) mRNA using T cells from one human donor. Each point denotes the mean % of mRNA remaining ± S.D.; *n* = 3. *F* and *H,* summary of the half-lives for IL-2 mRNA (*F*) and IFN-γ mRNA (*H*) for T cells from three human donors, and each *bar* denotes the mean half-life (min) ± S.D. for that donor; *, significantly different from vehicle-treated cells, *n* = 3. *ns,* not statistically significant.

of GRK2 through Tyr phosphorylation by an Src kinase. GRK2 then transactivates CXCR4 by phosphorylation of CXCR4–Ser-339, which is required for TCR–CXCR4 complex formation. TCR–CXCR4 complexes induce PREX1 localization to the plasma membrane via a mechanism requiring PI3Kγ. Activation of the PREX1 signaling pathway downstream of the TCR–CXCR4 complex results in mRNA stabilization and thus robust IL-2 and IL-10 production.

Discussion

We recently demonstrated that stimulation of the TCR results in the transactivation of CXCR4 and a physical interaction between the TCR and CXCR4. We showed that this allows CXCR4 to activate the PREX1/Rac-1 pathway and thereby enhance downstream IL-2 and IL-10 cytokine production (12). Here, we focused on characterizing the molecular mechanisms responsible for the formation of TCR–CXCR4 complexes that

Figure 10. PI3Kγ is required for TCR/CD3-induced IL-2 and IL-10 production by normal human T cells purified from peripheral blood. *A–E,* PBMC T cells isolated from healthy human donors were transfected with either control nontargeting siRNA, PI3Kγ siRNA #1, or PI3Kγ siRNA #2 and then cultured for 48 h. *A,* representative immunoblots demonstrating PI3Kγ depletion at 48 h. *B,* after the 48-h incubation, the cells were stimulated with 1 mg/ml plate-bound OKT3 and soluble CD28 for 24 h, and then apoptosis was assayed via annexin-V staining as in Fig. 3, *E and F*. Summary of results from four different blood donors is shown for each PI3Kγ siRNA; *bars* denote the mean % of primary T cells staining positive for annexin-V ± S.E.; *n* = 4. *C,* CXCR4 cell-surface expression was measured via flow cytometry 48 h after depletion of PI3Kγ via siRNAs. *Bars* denote the mean percentage of CXCR4 expression as compared with control siRNA-transfected cells analyzed the same day ± S.E.; *n* = 3. *D and E,* human PBMC T cells were depleted of PI3Kγ as above and were then stimulated with CD3 + CD28 mAb for an additional 24 h as in Fig. 3*H*. Culture supernatants were then assayed for cytokines as in Fig. 3*H*. *, significantly different from control cells; *p* < 0.05. *ns*, not statistically significant.

mediate activation of the PREX1 pathway required for IL-2 and IL-10 production. Our results identify GRK2 as critically required for TCR signaling to result in the transactivation of CXCR4 and the formation of TCR–CXCR4 complexes. We showed that GRK2 protein expression and kinase activity are both required for the TCR-induced phosphorylation of CXCR4–Ser-339 and for the subsequent formation of TCR–

CXCR4 complexes as detected via both FRET and proximity ligation assays. These results indicate that the expression and activity of GRK2 are both required for TCR signaling to result in robust cytokine production by normal human peripheral blood T cells, an outcome previously shown to be dependent on TCR signaling via TCR–CXCR4 complexes (12). Furthermore, we demonstrated that TCR coupling to this pathway requires
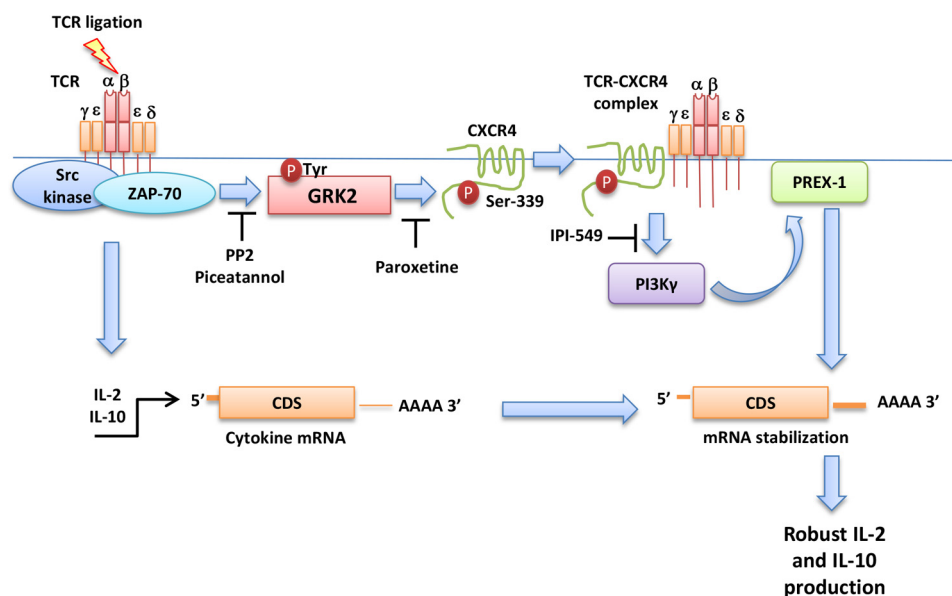
Figure 11. GRK2 mediates TCR-induced transactivation of CXCR4 and TCR–CXCR4 complex formation required for PI3Kγ/PREX1 signaling and robust T cell cytokine secretion. Our proposed model is that TCR/CD3 stimulation results in the activation of GRK2 through Tyr phosphorylation by an Src kinase. GRK2 then transactivates CXCR4 by phosphorylation of CXCR4–Ser-339, which drives TCR–CXCR4 complex formation. TCR–CXCR4 complexes induce PREX1 localization to the plasma membrane via a mechanism requiring PI3Kγ. Activation of the PREX1-signaling pathway downstream of the TCR–CXCR4 complex results in mRNA stabilization and thus robust IL-2 and IL-10 production.

upstream activation of Src kinases and ZAP-70, tyrosine kinases that associate with the activated TCR and mediate TCR signaling (14). We showed that TCR-stimulated Src kinase activity is required for inducible GRK2 tyrosine phosphorylation and for the GRK2-dependent events of TCR-stimulated phosphorylation of CXCR4 on Ser-339 and TCR–CXCR4 complex formation. Furthermore, we demonstrated that GRK2-mediated TCR–CXCR4 complex formation was required for the TCR to stimulate plasma membrane localization of PREX1 via PI3Kγ. We therefore characterized a novel role for PI3Kγ in mediating the mRNA stabilization of TCR-mediated IL-2 and IFN-γ transcripts. Together, our results characterize a previously unknown TCR-stimulated signaling pathway in which the TCR utilizes the TCR-associated tyrosine kinases to activate GRK2, which then phosphorylates CXCR4, thereby inducing formation of the TCR–CXCR4 heterodimers that mediate robust TCR-induced cytokine secretion via a PI3Kγ/PREX1 pathway.

In this study, we demonstrated that GRK2-mediated phosphorylation of CXCR4–Ser-339 is required for TCR–CXCR4 complex formation. Phosphorylation of CXCR4–Ser-339 most likely recruits one or more adaptor or scaffold proteins to the receptor that subsequently mediate signaling culminating in TCR–CXCR4 receptor complex formation. Phosphorylation of sites within the CXCR4 C-terminal region has previously been shown to recruit several scaffold proteins to the receptor, including β-arrestin 1 and 2, p52Shc, SHP2, Cbl, and drebrin (50–53); these or other scaffold proteins could play a role in mediating the physical association between the TCR and CXCR4. Alternatively or in addition, multiple scaffold and adapter proteins, including LAT, GADS, and SLP-76, participate in TCR signaling and could also be involved in mediating TCR–CXCR4 formation following GRK2 phosphorylation of CXCR4 (14).

By increasing understanding of the molecular mechanisms that regulate T cell-mediated cytokine production, the results described here could potentially lead to new therapies to regulate aberrant cytokine production in autoimmune diseases, allergies, and malignancies. IL-2 and IL-10 play crucial roles in modulating the immune response. IL-2 is necessary for T cell proliferation and differentiation; IL-2 is also important for induction of the T cell death mechanism, activation-induced cell death, that is essential for returning the immune system to homeostasis after a challenge by, for example, a viral infection (54). IL-10 is also a critical immune system regulator that is required for immune tolerance and provides balancing immunosuppression during inflammatory immune responses (55). Higher or lower levels of these and other cytokines are responsible for skewing the immune response toward a specific outcome, for example, by determining whether a particular immune response will be a Th1 (*e.g.* inflammatory) response *versus* a Th2 (*e.g.* allergic) response (56). Thus, our results indicate that the modulation of GRK2 expression and function in T cells could be a way to significantly regulate the immune response.

Antigen recognition receptor-mediated activation of GRK2 that results in the transactivation of a GPCR and receptor complex formation has not previously been described. Signaling from other GPCRs, RTKs, and antigen receptors has been demonstrated to form receptor heterodimers with or alter the activation state of CXCR4 through phosphorylation (19, 57). Stimulation of the GPCR CXCR7 results in CXCR7–CXCR4 complexes that allow CXCR7 to access β-arrestin and enhance chemotaxis (58). The RTKs EGFR, c-Kit, and IGF-1R have all been demonstrated to transactivate and use CXCR4 to couple to a variety of GPCR-dependent signaling pathways such as those that increase cell motility, tumorigenesis, MAPK signaling, β-arrestin–mediated signaling, and receptor desensitiza-

tion (23, 25–29). Stimulation of the B cell antigen receptor results in the desensitization of CXCR4 through phosphorylation (59). Thus, CXCR4, although ubiquitously expressed, can be used by different receptors in various cell types to activate distinct signaling pathways with specific outcomes. Our study characterizing the mechanisms by which the TCR utilizes GRK2 to transactivate and physically associate with CXCR4 may provide further insight into how other receptors might be transactivating and using CXCR4.

We report here that TCR signaling leads to rapid tyrosine phosphorylation of GRK2 via an Src kinase-dependent signaling pathway. Prior studies have demonstrated that phosphorylation of GRK2 at Tyr-13, Tyr-86, and Tyr-92 by Src kinases enhances GRK2 kinase activity (44, 60). Our results show that GRK2 is Tyr-phosphorylated by a TCR-activated Src kinase upon T cell activation. GRK2 has been previously shown to associate with the basal, unstimulated form of the TCR (41), which could bring GRK2 into proximity of TCR-induced Src kinases allowing the phosphorylation to occur. Alternatively, because we found that activation of another tyrosine kinase, ZAP-70, is also required for this pathway, Src kinases might also play an indirect role in activating GRK2 in response to TCR stimulation. TCR signaling is known to activate other tyrosine kinases that could also participate in activating GRK2 (61–63). Thus, TCR-mediated activation of Src kinases could lead to ZAP-70 activation, and ZAP-70 could then signal to either directly or indirectly phosphorylate and activate GRK2.

Our results suggest that blocking TCR–CXCR4 complex formation by targeting GRK2 might be useful in treating autoimmunity. Indeed, the selective GRK2 inhibitor paroxetine has been shown to reduce inflammation in rheumatoid arthritis (64, 65). Certain autoimmune diseases feature both elevated T cell cytokines and increased CXCR4 expression on pathogenic T cells (66, 67). It has been proposed that this elevated CXCR4 expression contributes to the increased T cell migration of these T cells into inflamed tissues (68, 69); the results in this paper additionally suggest that elevated CXCR4 might also significantly contribute to increased IL-2 production and thereby the increased proliferation of the pathogenic T cell clones. Thus, our further characterization of the signaling mechanisms that mediate a TCR-induced cytokine production may lead to novel therapies for immune diseases.

Experimental procedures

Materials

The following reagents were used: IPI-549 (Selleckchem); paroxetine (Sigma); PP2 and piceatannol (Calbiochem); fibronectin (BD Biosciences); anti-CXCR4 (clone 12G5, R&D Systems); biotinylated OKT3 (eBiosciences); anti-CD28, anti-CD3, anti-CXCR4, and avidin (BD Biosciences); anti-pTyr, clone 4G10 (Millipore); anti-GRK2 (ThermoFisher Scientific); and anti-phospho-CXCR4–Ser-339 (Abcam).

Cells

Jurkat T cells were maintained as described (10, 12). Normal human peripheral blood T cells (PBMC T cells) from anonymous healthy volunteers were isolated from peripheral blood with ~98% purity and maintained as described (10); this use of

human blood was approved by the Mayo Clinic Institutional Review Board.

FRET

Plasmids encoding WT–CXCR4–YFP, SS338/339AA–CXCR4–YFP, Δ322–CXCR4–YFP, and CD3ζ–CFP were previously described here (10, 34). FRET assays were performed as described previously (12). Briefly, Jurkat T cells were transiently transfected with plasmid expression constructs encoding the indicated tagged proteins, plus either 750 nmol of control siRNA or 750 nmol of GRK2 siRNA where indicated, and cultured for 16 h. Where indicated, transfected cells were treated with 0.1 μM paroxetine, vehicle (DMSO), 10 μM PP2, or 1 μM piceatannol for 30 min immediately prior to FRET analysis. TCR/CD3-stimulated TCR–CXCR4 complex formation was analyzed by FRET analysis as described previously (10–12). Fluorescent emission spectra in response to 433 nm light were measured using the Varioskan Flash (ThermoFisher Scientific) before and after CD3 stimulation via cross-linked CD3 mAb (OKT3). Percent change in YFP or CFP in response to CD3 stimulation was determined by calculating the difference in emission intensity over the CFP range (460–500 nm) or the YFP range (525–550 nm) and normalizing this change to the total fluorescence of the unstimulated sample.

PLA

PLA was performed as described (12). Jurkat T cells were transiently transfected with the indicated constructs as for the FRET experiments above, and cells were cultured for 16 h, pretreated with vehicle (DMSO), 10 μM PP2, or 1 μM piceatannol for 30 min where indicated, centrifuged onto coverslips coated with fibronectin and 1 μg/ml CD3 mAb (OKT3), and stimulated by incubation at 37 °C for 30 min. Cells were then fixed with 3% paraformaldehyde, permeabilized with 0.15% Triton Surface-amps (ThermoFisher Scientific), blocked with 5% BSA, 0.1% glycine, PBS, incubated overnight at 4 °C with goat anti-GFP and rabbit anti-CD3-ζ, and processed using the DUOLINK In SITU kit (Sigma). PLA was imaged using an LSM780 laser-scanning confocal microscope (Carl Zeiss) with a ×100/1.46 oil objective and laser/emission filter: 488/500–554 for CXCR4-YFP to identify transfected cells, 405/411–481 for 4',6-diamidino-2-phenylindole (DAPI) (blue), and 594/624 for PLA (red). ZEN software was used for imaging. FIJI was used to assess total PLA fluorescence.

CXCR4–Ser-339 phosphorylation assay

Jurkat T cells were transiently transfected with WT–CXCR4–YFP ± siRNA where indicated and cultured for 16 h. Cells were pretreated with 0.1 μM paroxetine, vehicle (DMSO), 10 μM PP2, or 1 μM piceatannol as indicated for 30 min immediately prior to CD3 stimulation. Cells were stimulated via CD3 mAb (OKT3)-biotin cross-linked with avidin for 5 min and then lysed with 1% Triton buffer. WT–CXCR4–YFP was immunoprecipitated using anti-GFP. Phosphorylation of CXCR4–Ser-339 was assayed by SDS-PAGE and immunoblotting with phospho-CXCR4–Ser-339 specific antisera (Abcam). As a control, the same blots were stripped and reprobed for total CXCR4 (R&D Systems).

Apoptosis assay

PBMC T cells from healthy donors were purified, transfected with the indicated siRNA, and then cultured for 48 h. Alternatively, PBMC T cells were pretreated with 3 μM paroxetine, 1 μM IPI-549, or vehicle (DMSO) for 1 h immediately prior to CD3 + CD28 stimulation. Cells were stimulated for 24 h with plate-bound CD3 mAb (OKT3) and 12.5 μg/ml soluble anti-CD28. Cells were harvested, stained with annexin V conjugated to allophycocyanin (APC), and analyzed by flow cytometry to detect cellular apoptosis.

Cytokine production assay

PBMC T cells from healthy donors were treated with 3 μM paroxetine, 1 μM IPI-549, or vehicle (DMSO). Alternatively, PBMC T cells were transiently transfected with 750 nM control siRNA (Dharmacon), GRK2 siRNA-1 (Dharmacon), GRK2 siRNA-2 (Ambion), PI3Kγ siRNA-1 (Dharmacon), and PI3Kγ siRNA-2 (Ambion) utilizing the human T cell nucleofector kit (Lonza) with program U-014. Human T cells were cultured for 48 h and then stimulated for 24 h with plate-bound 1 μg/ml CD3 mAb (OKT3) and 12.5 μg/ml soluble anti-CD28. Culture supernatants were harvested, and cytokine production was analyzed via ELISA (BD Biosciences).

GRK2 Tyr phosphorylation assay

Jurkat T cells were pretreated with either 10 μM PP2 or vehicle (DMSO) and then stimulated with CD3 mAb (OKT3-biotin) and cross-linked with avidin for the indicated time. Endogenous GRK2 was immunoprecipitated with GRK-2 antibody (ThermoFisher Scientific) and analyzed by SDS-PAGE and immunoblotting with anti-phosphotyrosine (clone 4G10; Millipore). As a control, the same blots were stripped and reprobed with total GRK2 antisera (ThermoFisher Scientific).

PREX1 localization assay

Plasmids encoding eGFP-PREX1 were generously provided by Dr. Heidi Welch (Babraham Institute) (48, 49). Jurkat T cells were transiently transfected with eGFP-PREX1 and cultured overnight. Cells were pretreated with 0.1 μM paroxetine, 1.0 μM IPI-549, or vehicle (DMSO). The cells were stimulated, fixed, permeabilized, and mounted as described for the PLA above. Cells were imaged using an LSM780 laser-scanning confocal microscope (Carl Zeiss) with a $\times$100/1.46 oil objective and laser/emission filter: 488/500–554 for eGFP-PREX1 to identify transfected cells and 405/411–481 for DAPI (blue). ZEN software was used for imaging. FIJI was used to assess membrane localization. Fluorescence profile was generated along an axis through the cell. Fluorescence intensity at the cell membrane and total fluorescence along the axis were used to calculated percent of PREX1 localized to the membrane.

IL-2 luciferase assay

IL-2 luciferase activity was assayed as described previously (10, 70). Briefly, Jurkat T cells were transfected with the 585– IL-2 promoter luciferase construct and cultured overnight. Cells were treated with DMSO or 1.0 μM IPI-549 for 1 h and then stimulated with plate-bound OKT3 and soluble anti-CD28 for 24 h. Cells were harvested and lysed, and luciferase activity was measured.

mRNA stability assay

To measure mRNA stability, cells were treated with DMSO and 1.0 μM IPI-549 1 h prior to stimulation. PBMC T cells were stimulated with plate-bound CD3 mAb (OKT3) and soluble anti-CD28 for 5.5 h and then treated with 8 μg/ml actinomycin D for the indicated time. mRNA was reverse-transcribed via iScript cDNA synthesis kit (Bio-Rad) and measured via RT^2 SYBR Green Fluor qRT-PCR (Qiagen) on Light Cycler 480 (Roche Applied Science) utilizing PrimeTime quantitative PCR primer sets (IDT). Transcript levels were normalized to GAPDH and quantified using the $2^{\Delta\Delta Ct}$ method.

References

1. Siebert, S., Tsoukas, A., Robertson, J., and McInnes, I. (2015) Cytokines as therapeutic targets in rheumatoid arthritis and other inflammatory diseases. *Pharmacol. Rev.* **67,** 280–309 CrossRef Medline
2. Rubio Gonzalez, B., Zain, J., Rosen, S. T., and Querfeld, C. (2016) Tumor microenvironment in mycosis fungoides and Sezary syndrome. *Curr. Opin. Oncol.* **28,** 88–96 CrossRef Medline
3. Huang, W., and August, A. (2015) The signaling symphony: T cell receptor tunes cytokine-mediated T cell differentiation. *J. Leukoc. Biol.* **97,** 477–485 CrossRef Medline
4. Bromley, S. K., and Dustin, M. L. (2002) Stimulation of naive T-cell adhesion and immunological synapse formation by chemokine-dependent and -independent mechanisms. *Immunology* **106,** 289–298 CrossRef Medline
5. Trampont, P. C., Tosello-Trampont, A. C., Shen, Y., Duley, A. K., Sutherland, A. E., Bender, T. P., Littman, D. R., and Ravichandran, K. S. (2010) CXCR4 acts as a costimulator during thymic β-selection. *Nat. Immunol.* **11,** 162–170 CrossRef Medline
6. Cascio, G., Martín-Cófreces, N. B., Rodríguez-Frade, J. M., López-Cotarelo, P., Criado, G., Pablos, J. L., Rodriguez-Fernandez, J. L., Sánchez-Madrid, F., and Mellado, M. (2015) CXCL12 regulates through JAK1 and JAK2 formation of productive immunological synapses. *J. Immunol.* **194,** 5509–5519 CrossRef Medline
7. Smith, X., Schneider, H., Köhler, K., Liu, H., Lu, Y., and Rudd, C. E. (2013) The chemokine CXCL12 generates costimulatory signals in T cells to enhance phosphorylation and clustering of the adaptor protein SLP-76. *Sci. Signal.* **6,** ra65 Medline
8. Kremer, K. N., Humphreys, T. D., Kumar, A., Qian, N. X., and Hedin, K. E. (2003) Distinct role of ZAP-70 and Src homology 2 domain-containing leukocyte protein of 76 kDa in the prolonged activation of extracellular signal-regulated protein kinase by the stromal cell-derived factor-1 α/CXCL12 chemokine. *J. Immunol.* **171,** 360–367 CrossRef Medline
9. Kremer, K. N., Kumar, A., and Hedin, K. E. (2007) Haplotype-independent costimulation of IL-10 secretion by SDF-1/CXCL12 proceeds via AP-1

binding to the human IL-10 promoter. *J. Immunol.* **178,** 1581–1588 CrossRef Medline

10. Kumar, A., Humphreys, T. D., Kremer, K. N., Bramati, P. S., Bradfield, L., Edgar, C. E., and Hedin, K. E. (2006) CXCR4 physically associates with the T cell receptor to signal in T cells. *Immunity* **25,** 213–224 CrossRef Medline

11. Kumar, A., Kremer, K. N., Sims, O. L., and Hedin, K. E. (2009) Measuring the proximity of T-lymphocyte CXCR4 and TCR by fluorescence resonance energy transfer (FRET). *Methods Enzymol.* **460,** 379–397 CrossRef Medline

12. Kremer, K. N., Dinkel, B. A., Sterner, R. M., Osborne, D. G., Jevremovic, D., and Hedin, K. E. (2017) TCR–CXCR4 signaling stabilizes cytokine mRNA transcripts via a PREX1-Rac1 pathway: implications for CTCL. *Blood* **130,** 982–994 CrossRef Medline

13. Masopust, D., and Schenkel, J. M. (2013) The integration of T cell migration, differentiation and function. *Nat. Rev. Immunol.* **13,** 309–320 CrossRef Medline

14. Gorentla, B. K., and Zhong, X. P. (2012) T cell receptor signal transduction in T lymphocytes. *J. Clin. Cell. Immunol.* 2012, (Suppl. 12) 5

15. Maekawa, T., and Ishii, T. (2000) Chemokine/receptor dynamics in the regulation of hematopoiesis. *Intern. Med.* **39,** 90–100 CrossRef Medline

16. Nagasawa, T., Tachibana, K., and Kishimoto, T. (1998) A novel CXC chemokine PBSF/SDF-1 and its receptor CXCR4: their functions in development, hematopoiesis and HIV infection. *Semin. Immunol.* **10,** 179–185 CrossRef Medline

17. Przybyla, J. A., and Watts, V. J. (2010) Ligand-induced regulation and localization of cannabinoid CB1 and dopamine D2L receptor heterodimers. *J. Pharmacol. Exp. Ther.* **332,** 710–719 CrossRef Medline

18. Isik, N., Hereld, D., and Jin, T. (2008) Fluorescence resonance energy transfer imaging reveals that chemokine-binding modulates heterodimers of CXCR4 and CCR5 receptors. *PLoS ONE* **3,** e3424 CrossRef Medline

19. Delcourt, N., Bockaert, J., and Marin, P. (2007) GPCR-jacking: from a new route in RTK signalling to a new concept in GPCR activation. *Trends Pharmacol. Sci.* **28,** 602–607 CrossRef Medline

20. Vila-Coro, A. J., Rodríguez-Frade, J. M., Martín De Ana, A., Moreno-Ortíz, M. C., Martínez-A., C., and Mellado, M. (1999) The chemokine SDF-1α triggers CXCR4 receptor dimerization and activates the JAK/STAT pathway. *FASEB J.* **13,** 1699–1710 CrossRef Medline

21. Rodríguez-Frade, J. M., Vila-Coro, A. J., de Ana, A. M., Albar, J. P., Martínez, A. C., and Mellado, M. (1999) The chemokine monocyte chemoattractant protein-1 induces functional responses through dimerization of its receptor CCR2. *Proc. Natl. Acad. Sci. U.S.A.* **96,** 3628–3633 CrossRef Medline

22. Rodríguez-Frade, J. M., Vila-Coro, A. J., Martín, A., Nieto, M., Sánchez-Madrid, F., Proudfoot, A. E., Wells, T. N., Martínez, A. C., and Mellado, M. (1999) Similarities and differences in RANTES- and (AOP)-RANTES-triggered signals: implications for chemotaxis. *J. Cell Biol.* **144,** 755–765 CrossRef Medline

23. Akekawatchai, C., Holland, J. D., Kochetkova, M., Wallace, J. C., and McColl, S. R. (2005) Transactivation of CXCR4 by the insulin-like growth factor-1 receptor (IGF-1R) in human MDA-MB-231 breast cancer epithelial cells. *J. Biol. Chem.* **280,** 39701–39708 CrossRef Medline

24. Sosa, M. S., Lopez-Haber, C., Yang, C., Wang, H., Lemmon, M. A., Busillo, J. M., Luo, J., Benovic, J. L., Klein-Szanto, A., Yagi, H., Gutkind, J. S., Parsons, R. E., and Kazanietz, M. G. (2010) Identification of the Rac–GEF P-Rex1 as an essential mediator of ErbB signaling in breast cancer. *Mol. Cell* **40,** 877–892 CrossRef Medline

25. Zuo, K., Kuang, D., Wang, Y., Xia, Y., Tong, W., Wang, X., Chen, Y., Duan, Y., and Wang, G. (2016) SCF/c-kit transactivates CXCR4-serine 339 phosphorylation through G protein-coupled receptor kinase 6 and regulates cardiac stem cell migration. *Sci. Rep.* **6,** 26812 CrossRef Medline

26. Haribabu, B., Richardson, R. M., Fisher, I., Sozzani, S., Peiper, S. C., Horuk, R., Ali, H., and Snyderman, R. (1997) Regulation of human chemokine receptors CXCR4. Role of phosphorylation in desensitization and internalization. *J. Biol. Chem.* **272,** 28726–28731 CrossRef Medline

27. Mueller, W., Schütz, D., Nagel, F., Schulz, S., and Stumm, R. (2013) Hierarchical organization of multi-site phosphorylation at the CXCR4 C terminus. *PLoS ONE* **8,** e64975 CrossRef Medline

28. Brault, L., Rovó, A., Decker, S., Dierks, C., Tzankov, A., and Schwaller, J. (2014) CXCR4-SERINE339 regulates cellular adhesion, retention and mobilization, and is a marker for poor prognosis in acute myeloid leukemia. *Leukemia* **28,** 566–576 CrossRef Medline

29. Santio, N. M., Eerola, S. K., Paatero, I., Yli-Kauhaluoma, J., Anizon, F., Moreau, P., Tuomela, J., Härkönen, P., and Koskinen, P. J. (2015) Pim kinases promote migration and metastatic growth of prostate cancer xenografts. *PLoS ONE* **10,** e0130340 CrossRef Medline

30. Busillo, J. M., Armando, S., Sengupta, R., Meucci, O., Bouvier, M., and Benovic, J. L. (2010) Site-specific phosphorylation of CXCR4 is dynamically regulated by multiple kinases and results in differential modulation of CXCR4 signaling. *J. Biol. Chem.* **285,** 7805–7817 CrossRef Medline

31. Yang, J., Villar, V. A., Armando, I., Jose, P. A., and Zeng, C. (2016) G protein-coupled receptor kinases: crucial regulators of blood pressure. *J. Am. Heart Assoc.* **5,** e003519 CrossRef Medline

32. De Blasi, A., Parruti, G., and Sallese, M. (1995) Regulation of G protein-coupled receptor kinase subtypes in activated T lymphocytes. Selective increase of β-adrenergic receptor kinase 1 and 2. *J. Clin. Invest.* **95,** 203–210 CrossRef Medline

33. Welch, H. C. (2015) Regulation and function of P-Rex family Rac–GEFs. *Small GTPases* **6,** 49–70 CrossRef Medline

34. Hawkins, P. T., and Stephens, L. R. (2015) PI3K signalling in inflammation. *Biochim Biophys Acta* **1851,** 882–897 CrossRef Medline

35. Stark, A. K., Sriskantharajah, S., Hessel, E. M., and Okkenhaug, K. (2015) PI3K inhibitors in inflammation, autoimmunity and cancer. *Curr. Opin. Pharmacol.* **23,** 82–91 CrossRef Medline

36. Patton, D. T., Garçon, F., and Okkenhaug, K. (2007) The PI3K p110δ controls T-cell development, differentiation and regulation. *Biochem. Soc. Trans.* **35,** 167–171 CrossRef Medline

37. Orsini, M. J., Parent, J. L., Mundell, S. J., Marchese, A., and Benovic, J. L. (1999) Trafficking of the HIV coreceptor CXCR4. Role of arrestins and identification of residues in the C-terminal tail that mediate receptor internalization. *J. Biol. Chem.* **274,** 31076–31086 CrossRef Medline

38. Amara, A., Gall, S. L., Schwartz, O., Salamero, J., Montes, M., Loetscher, P., Baggiolini, M., Virelizier, J. L., and Arenzana-Seisdedos, F. (1997) HIV coreceptor downregulation as antiviral principle: SDF-1α-dependent internalization of the chemokine receptor CXCR4 contributes to inhibition of HIV replication. *J. Exp. Med.* **186,** 139–146 CrossRef Medline

39. Clift, I. C., Bamidele, A. O., Rodriguez-Ramirez, C., Kremer, K. N., and Hedin, K. E. (2014) β-Arrestin1 and distinct CXCR4 structures are required for stromal derived factor-1 to downregulate CXCR4 cell-surface levels in neuroblastoma. *Mol. Pharmacol.* **85,** 542–552 CrossRef Medline

40. Gupta, S. K., Lysko, P. G., Pillarisetti, K., Ohlstein, E., and Stadel, J. M. (1998) Chemokine receptors in human endothelial cells. Functional expression of CXCR4 and its transcriptional regulation by inflammatory cytokines. *J. Biol. Chem.* **273,** 4282–4287 CrossRef Medline

41. DeFord-Watts, L. M., Young, J. A., Pitcher, L. A., and van Oers, N. S. (2007) The membrane-proximal portion of CD3 epsilon associates with the serine/threonine kinase GRK2. *J. Biol. Chem.* **282,** 16126–16134 CrossRef Medline

42. Thal, D. M., Homan, K. T., Chen, J., Wu, E. K., Hinkle, P. M., Huang, Z. M., Chuprun, J. K., Song, J., Gao, E., Cheung, J. Y., Sklar, L. A., Koch, W. J., and Tesmer, J. J. (2012) Paroxetine is a direct inhibitor of G protein-coupled receptor kinase 2 and increases myocardial contractility. *ACS Chem. Biol.* **7,** 1830–1839 CrossRef Medline

43. Guccione, M., Ettari, R., Taliani, S., Da Settimo, F., Zappalà, M., and Grasso, S. (2016) G-protein-coupled receptor kinase 2 (GRK2) inhibitors: current trends and future perspectives. *J. Med. Chem.* **59,** 9277–9294 CrossRef Medline

44. Sarnago, S., Elorza, A., and Mayor, F., Jr. (1999) Agonist-dependent phosphorylation of the G protein-coupled receptor kinase 2 (GRK2) by Src tyrosine kinase. *J. Biol. Chem.* **274,** 34411–34416 CrossRef Medline

45. Iwashima, M., Irving, B. A., van Oers, N. S., Chan, A. C., and Weiss, A. (1994) Sequential interactions of the TCR with two distinct cytoplasmic tyrosine kinases. *Science* **263,** 1136–1139 CrossRef Medline

46. van Oers, N. S., Killeen, N., and Weiss, A. (1996) Lck regulates the tyrosine phosphorylation of the T cell receptor subunits and ZAP-70 in murine thymocytes. *J. Exp. Med.* **183,** 1053–1062 CrossRef Medline

ASBMB

47. Hanke, J. H., Gardner, J. P., Dow, R. L., Changelian, P. S., Brissette, W. H., Weringer, E. J., Pollok, B. A., and Connelly, P. A. (1996) Discovery of a novel, potent, and Src family-selective tyrosine kinase inhibitor. Study of Lck- and FynT-dependent T cell activation. *J. Biol. Chem.* **271,** 695–701 CrossRef Medline

48. Pan, D., Barber, M. A., Hornigold, K., Baker, M. J., Toth, J. M., Oxley, D., and Welch, H. C. (2016) Norbin stimulates the catalytic activity and plasma membrane localization of the guanine-nucleotide exchange factor P-Rex1. *J. Biol. Chem.* **291,** 6359–6375 CrossRef Medline

49. Welch, H. C., Coadwell, W. J., Ellson, C. D., Ferguson, G. J., Andrews, S. R., Erdjument-Bromage, H., Tempst, P., Hawkins, P. T., and Stephens, L. R. (2002) P-Rex1, a PtdIns(3,4,5)P$_3$- and G$\beta\gamma$-regulated guanine-nucleotide exchange factor for Rac. *Cell* **108,** 809–821 CrossRef Medline

50. Rocha-Perugini, V., Gordon-Alonso, M., and Sánchez-Madrid, F. (2017) Role of Drebrin at the immunological synapse. *Adv. Exp. Med. Biol.* **1006,** 271–280 CrossRef Medline

51. Patrussi, L., Ulivieri, C., Lucherini, O. M., Paccani, S. R., Gamberucci, A., Lanfrancone, L., Pelicci, P. G., and Baldari, C. T. (2007) P52Shc is required for CXCR4-dependent signaling and chemotaxis in T cells. *Blood* **110,** 1730–1738 CrossRef Medline

52. Chernock, R. D., Cherla, R. P., and Ganju, R. K. (2001) SHP2 and CBL participate in α-chemokine receptor CXCR4-mediated signaling pathways. *Blood* **96,** 608–615

53. Magalhaes, A. C., Dunn, H., and Ferguson, S. S. (2012) Regulation of GPCR activity, trafficking and localization by GPCR-interacting proteins. *Br. J. Pharmacol.* **165,** 1717–1736 CrossRef Medline

54. Boyman, O., and Sprent, J. (2012) The role of interleukin-2 during homeostasis and activation of the immune system. *Nat. Rev. Immunol.* **12,** 180–190 CrossRef Medline

55. Sabat, R., Grütz, G., Warszawska, K., Kirsch, S., Witte, E., Wolk, K., and Geginat, J. (2010) Biology of interleukin-10. *Cytokine Growth Factor Rev.* **21,** 331–344 CrossRef Medline

56. Borish, L. C., and Steinke, J. W. (2003) Cytokines and chemokines. *J. Allergy Clin. Immunol.* **111,** S460–75 CrossRef Medline

57. Pyne, N. J., and Pyne, S. (2011) Receptor tyrosine kinase–G-protein-coupled receptor signalling platforms: out of the shadow? *Trends Pharmacol. Sci.* **32,** 443–450 CrossRef Medline

58. Décaillot, F. M., Kazmi, M. A., Lin, Y., Ray-Saha, S., Sakmar, T. P., and Sachdev, P. (2011) CXCR7/CXCR4 heterodimer constitutively recruits β-arrestin to enhance cell migration. *J. Biol. Chem.* **286,** 32188–32197 CrossRef Medline

59. Chen, S. S., Chang, B. Y., Chang, S., Tong, T., Ham, S., Sherry, B., Burger, J. A., Rai, K. R., and Chiorazzi, N. (2016) BTK inhibition results in impaired CXCR4 chemokine receptor surface expression, signaling and function in chronic lymphocytic leukemia. *Leukemia* **30,** 833–843 CrossRef Medline

60. Penela, P., Ribas, C., and Mayor, F., Jr. (2003) Mechanisms of regulation of the expression and function of G protein-coupled receptor kinases. *Cell. Signal.* **15,** 973–981 CrossRef Medline

61. Krasel, C., Dammeier, S., Winstel, R., Brockmann, J., Mischak, H., and Lohse, M. J. (2001) Phosphorylation of GRK2 by protein kinase C abolishes its inhibition by calmodulin. *J. Biol. Chem.* **276,** 1911–1915 CrossRef Medline

62. Li, X., Huston, E., Lynch, M. J., Houslay, M. D., and Baillie, G. S. (2006) Phosphodiesterase-4 influences the PKA phosphorylation status and membrane translocation of G-protein receptor kinase 2 (GRK2) in HEK-293β2 cells and cardiac myocytes. *Biochem. J.* **394,** 427–435 CrossRef Medline

63. Murthy, K. S., Mahavadi, S., Huang, J., Zhou, H., and Sriwai, W. (2008) Phosphorylation of GRK2 by PKA augments GRK2-mediated phosphorylation, internalization, and desensitization of VPAC2 receptors in smooth muscle. *Am. J. Physiol. Cell Physiol.* **294,** C477–C487 CrossRef Medline

64. Wang, Q., Wang, L., Wu, L., Zhang, M., Hu, S., Wang, R., Han, Y., Wu, Y., Zhang, L., Wang, X., Sun, W., and Wei, W. (2017) Paroxetine alleviates T lymphocyte activation and infiltration to joints of collagen-induced arthritis. *Sci. Rep.* **7,** 45364 CrossRef Medline

65. Bird, H., and Broggini, M. (2000) Paroxetine versus amitriptyline for treatment of depression associated with rheumatoid arthritis: a randomized, double blind, parallel group study. *J. Rheumatol.* **27,** 2791–2797 Medline

66. Nanki, T., Hayashida, K., El-Gabalawy, H. S., Suson, S., Shi, K., Girschick, H. J., Yavuz, S., and Lipsky, P. E. (2000) Stromal cell-derived factor-1-CXC chemokine receptor 4 interactions play a central role in CD4+ T cell accumulation in rheumatoid arthritis synovium. *J. Immunol.* **165,** 6590–6598 CrossRef Medline

67. Launay, O., Paul, S., Servettaz, A., Roguet, G., Rozenberg, F., Lucht, F., Lambert, C., Presles, E., Goulvestre, C., Méritet, J. F., Galtier, F., Dubray, C., Lebon, P., Weill, B., and Batteux, F. (2013) Control of humoral immunity and auto-immunity by the CXCR4/CXCL12 axis in lupus patients following influenza vaccine. *Vaccine* **31,** 3492–3501 CrossRef Medline

68. Kohler, R. E., Comerford, I., Townley, S., Haylock-Jacobs, S., Clark-Lewis, I., and McColl, S. R. (2008) Antagonism of the chemokine receptors CXCR3 and CXCR4 reduces the pathology of experimental autoimmune encephalomyelitis. *Brain Pathol.* **18,** 504–516 Medline

69. Buckley, C. D., Amft, N., Bradfield, P. F., Pilling, D., Ross, E., Arenzana-Seisdedos, F., Amara, A., Curnow, S. J., Lord, J. M., Scheel-Toellner, D., and Salmon, M. (2000) Persistent induction of the chemokine receptor CXCR4 by TGF-β1 on synovial T cells contributes to their accumulation within the rheumatoid synovium. *J. Immunol.* **165,** 3423–3429 CrossRef Medline

70. Macián, F., García-Rodríguez, C., and Rao, A. (2000) Gene expression elicited by NFAT in the presence or absence of cooperative recruitment of Fos and Jun. *EMBO J.* **19,** 4783–4795 CrossRef Medline